

# MAGNETIC OPTICS CALCULATIONS FOR CYLINDRICALLY SYMMETRIC BEAMS WITH SPACE CHARGE

ROBERT D. RYNE\*

*Beam Research Program, L-626, Lawrence Livermore National Laboratory,  
Livermore, CA 94550, USA.*

and

ALEX J. DRAGT†

*Department of Physics and Astronomy, University of Maryland, College Park,  
MD 20742, USA.*

*(Received 20 April 1990; in final form 14 August 1990)*

The purpose of this report is to discuss a new approach for doing magnetic optics calculations in the presence of space charge. Our approach is based on the self-consistent calculation of the transfer map,  $\mathcal{M}$ , that describes the motion of individual particles. Since our approach is based on the computation of  $\mathcal{M}$ , it is the only method that provides for the *direct* calculation of aberrations in beam transport systems with space charge. In this report, we will treat cylindrically symmetric beams in beam transport systems consisting of drifts and solenoids. We will derive ordinary differential equations for a third order representation of  $\mathcal{M}$ . We will show how this formalism can be used to predict rms beam size and emittance growth caused by nonlinear optical effects and nonlinear space charge effects. Since our method does not rely on “pushing particles,” it is much faster than particle simulation. (However, it is not as generally applicable as particle simulation.) As a specific example, we will consider the focusing of a cold beam by a solenoid. We will show that predictions of beam evolution based on our method are in good agreement with particle simulation.

## 1 INTRODUCTION

The purpose of this report is to discuss a new method for doing magnetic optics calculations in the presence of space charge. Our approach is based on the self-consistent calculation of the transfer map,  $\mathcal{M}$ , that describes the motion of individual particles. To simplify the analysis, we will restrict our attention to systems with cylindrical symmetry; however, this approach can be used to analyze other beam transport systems. We will consider the propagation of beams with space charge in

---

\* Work performed under the auspices of the U.S. Department of Energy by Lawrence Livermore National Laboratory under contract W-7405-ENG-48.

† Work supported in part under the U.S. Department of Energy contract DE-AS05-80ER10666.

beam transport systems consisting of drifts and solenoids, subject to the following approximations:

- 1) We will assume that a cylindrically symmetric beam is launched along the axis of a perfectly aligned beam transport system.
- 2) We will perform a two-dimensional analysis. We will assume that the beam is infinitely long, and we will only analyze the transverse beam dynamics.
- 3) We will neglect the longitudinal electric field,  $E_z$ , associated with space charge.
- 4) We will assume that all particles have the same total energy.
- 5) We will neglect image charge effects.

Our analysis will include nonlinear effects through third order. We will derive ordinary differential equations for a third-order representation of  $\mathcal{M}$ . We will show how this formalism can be used to predict rms beam size and emittance growth caused by nonlinear optical effects and nonlinear space charge effects. As a specific example, we will consider the focusing of a cold beam by a solenoid. We will show that predictions of beam evolution based on this method are in good agreement with particle simulation. Since our method does not rely on “pushing particles”, it is much faster than particle simulation. (However, it is not as generally applicable as particle simulation.) Furthermore, it provides for the *direct* computation of optical quantities such as aberration coefficients, since they are simply related to the coefficients of  $\mathcal{M}$ .

## 2 STATEMENT OF THE PROBLEM

Consider a particle beam in a beam transport system consisting of drifts and solenoids. In general, this is a three-dimensional problem. However, eventually we will treat just the two-dimensional problem of calculating the transverse beam dynamics as a function of the longitudinal coordinate  $z$ . We will show that the transverse motion is governed by some Hamiltonian,  $H(x, p_x, y, p_y; z)$ . Let  $\zeta$  denote the collection of coordinates and momenta,  $\zeta = (x, p_x, y, p_y)$ . Let  $z^i$  denote some initial position and let  $z^f$  denote some final position. We shall use the notation  $\zeta^i = \zeta(z^i)$  and  $\zeta^f = \zeta(z^f)$ . We may regard the beam transport system as being governed by some (generally nonlinear) mapping,  $\mathcal{M}$ , where  $\mathcal{M}$  has the property that

$$\zeta^f = \mathcal{M}\zeta^i. \quad (1)$$

The transfer map  $\mathcal{M}$  depends on  $z^i$  and  $z^f$ , but to simplify the notation we shall write  $\mathcal{M}$  instead of  $\mathcal{M}(z^i, z^f)$ .

Now suppose that the particle beam is characterized by a distribution function,  $f(\zeta, z)$ , with initial value

$$f(\zeta, z^i) = f^o(\zeta), \quad (2)$$

and suppose that  $f$  satisfies the Vlasov equation,

$$\frac{d}{dz} f(\zeta, z) = 0, \quad (3)$$

where  $d/dz$  denotes the total derivative with respect to  $z$ . Then it is easy to show that the  $z$ -dependent distribution function is given by

$$f(\zeta, z) = f^o(\mathcal{M}^{-1}\zeta). \quad (4)$$

(Note that the  $z$  dependence of the solution is contained in  $\mathcal{M}^{-1}$ .) Since  $\mathcal{M}$  determines the evolution of the particle beam, we will concentrate on calculating  $\mathcal{M}$ .

### 3 SELF-CONSISTENT TRANSFER MAPS

Transfer map methods have been widely used in the design, optimization and evaluation of beam transport systems without space charge. For example, the codes TRANSPORT<sup>1</sup> and MAD<sup>2</sup> are used extensively in the United States and Europe, respectively. These codes represent the trajectories of particles near some design trajectory using a Taylor series,

$$\zeta_a^f = \sum_{b=1}^4 M_{ab} \zeta_b^i + \sum_{1 \leq b \leq c}^4 T_{abc} \zeta_b^i \zeta_c^i + \sum_{1 \leq b \leq c \leq d}^4 U_{abcd} \zeta_b^i \zeta_c^i \zeta_d^i + \dots \quad (5)$$

(For a three-dimensional problem, the above summations would run from 1 to 6.) The matrix  $M$  determines the linear (or paraxial or ‘‘Gaussian’’) behavior of the system; the tensors  $T$  and  $U$  describe nonlinear effects of order 2 and 3, respectively. Another popular approach is the use of Lie algebraic methods to represent transfer maps. Instead of the tensors  $T$ ,  $U$ , etc., this approach utilizes certain polynomials to describe nonlinear effects. The widely used code MARYLIE 3.0 is based on Lie algebraic methods.<sup>3</sup>

The quantities  $M$ ,  $T$ , and  $U$  (and their Lie algebraic analogues) can be determined analytically for ‘‘ideal’’ beamline elements: drifts, dipoles, quadrupoles (including ‘‘hard edge’’ fringe fields), sextupoles and octupoles, for example. It is important to note that these quantities can be computed numerically for non-ideal beamline elements, such as dipoles and quadrupoles with ‘‘real’’ fringe fields. In other words, there are standard tools available for the numerical computation of transfer maps of  $z$ -dependent beamline elements.<sup>4,5,6,7</sup> All that is required is a knowledge of the Hamiltonian (or, equivalently, the electromagnetic fields) for the beam transport system in question.

So far, the discussion has been limited to beam transport systems without space charge. Now consider beam transport systems with space charge. Our approach is based on the fact that a beam with space charge, propagating in some beam transport system, may be viewed as a ‘‘special’’ beam transport system with  $z$ -dependent fields. It is special because the  $z$ -dependent fields are due (at least partly) to the beam self-fields. Thus, the  $z$ -dependent fields in the problem are not known *a priori*. If we could obtain an expression for the beam self-fields, we could use the standard tools for obtaining transfer maps of  $z$ -dependent beamline elements.

The solution to our dilemma is to calculate the beam self-fields in terms of the unknown mapping  $\mathcal{M}$  and the initial distribution function. Namely, the  $z$ -dependent

charge density (which determines the self-fields in the electrostatic approximation) is given by

$$\rho(\mathbf{x}; z) = Q \int d\mathbf{p} f(\zeta, z) = Q \int d\mathbf{p} f^o(\mathcal{M}^{-1}\zeta), \quad (6)$$

where  $Q$  is the total charge of the distribution of particles. Alternatively, we can write down a formal expression for the scalar potential directly. In two dimensions,

$$\psi(x, y; z) = \frac{\lambda_q}{(2\pi)^2 \epsilon_0} \int d^4\zeta' \int d^2k \frac{1}{k^2} e^{ik_x(x-x')} e^{ik_y(y-y')} f^o(\mathcal{M}^{-1}\zeta'), \quad (7)$$

where  $\lambda_q$  denotes the charge per unit length. There are two facts about this equation worth noting:

1) This equation need not be solved exactly. Generally, the mapping  $\mathcal{M}$  is calculated through some given order. The evaluation of the above integral expression should be consistent with that approximation. In particular, we will calculate  $\psi$  as a power series in  $x$  and  $y$ . (We will arbitrarily set the constant term in the series expansion of  $\psi$  equal to zero; the singularity in Eq. (7) at  $k = 0$  presents no difficulty in calculating the remaining terms.)

2) The evaluation of the above equation is very tedious. The reason is that the quantity  $\mathcal{M}$  contains many coefficients. Thus, it is worthwhile to represent  $\mathcal{M}$  by a method that utilizes the minimum number of coefficients. We shall use a Lie algebraic representation, as will be described later.

Eq. (7) is a self-consistent formula for the scalar potential in terms of the unknown mapping  $\mathcal{M}$ . We shall use this formula in our expression for the Hamiltonian of the system. Since the Hamiltonian includes the self-consistent scalar potential, we call  $\mathcal{M}$  a *self-consistent transfer map*. Finally, since  $\mathcal{M}$  is a function of  $z$ , it follows that self fields in our problem are generally  $z$ -dependent.

Now we can use the standard tools that have been developed for the numerical computation of transfer maps corresponding to  $z$ -dependent beamline elements. To perform such calculations, we need to compute the Hamiltonian for the beam transport system, and we need to expand the Hamiltonian around the design orbit. This is the subject of the next section.

#### 4 CALCULATION OF THE HAMILTONIAN

We begin with the relativistic Hamiltonian in MKSA units for a particle of charge  $q$  and mass  $m$ :

$$H = \sqrt{m^2 c^4 + c^2 [(p_x - qA_x)^2 + (p_y - qA_y)^2 + (p_z - qA_z)^2]} + q\psi(x, y, z, t), \quad (8)$$

where

$$\begin{aligned} \mathbf{B} &= \nabla \times \mathbf{A}, \\ \mathbf{E} &= -\nabla\psi - \frac{\partial \mathbf{A}}{\partial t}. \end{aligned} \quad (9)$$

Now we will make several transformations of this Hamiltonian: First we will make  $z$  the independent variable; next we will scale the phase space variables to obtain dimensionless quantities; lastly we will obtain new variables that are deviations from the design trajectory. (Throughout this process, we will use the symbols  $H$  and  $K$  to denote various Hamiltonians).

Following the usual procedure, we can make  $z$  the independent variable. First set  $p_t = -H$  and solve for  $p_z$ . Then set  $K = -p_z$ . The quantity  $K$  is the new Hamiltonian with  $z$  as the independent variable:

$$K(x, p_x, y, p_y, t, p_t; z) = -\sqrt{(p_t + q\psi)^2/c^2 - m^2c^2 - (p_x - qA_x)^2 - (p_y - qA_y)^2} - qA_z(x, y, t; z). \quad (10)$$

Next, define dimensionless variables by the rules

$$\begin{aligned} \bar{x} &= x/l, & \bar{p}_x &= p_x/p^o, \\ \bar{y} &= y/l, & \bar{p}_y &= p_y/p^o, \\ \bar{t} &= \frac{t}{l/c}, & \bar{p}_t &= \frac{p_t}{p^o c}, \end{aligned} \quad (11)$$

where  $l$  is any (scale) length and  $p^o$  is any (scale) momentum. These dimensionless variables are governed by the following Hamiltonian:

$$\tilde{K}(\bar{x}, \bar{p}_x, \bar{y}, \bar{p}_y, \bar{t}, \bar{p}_t; z) = -\frac{1}{l} \sqrt{\left(\bar{p}_t + \frac{q\psi}{p^o c}\right)^2 - \left(\frac{mc}{p^o}\right)^2 - \left(\bar{p}_x - \frac{q}{p^o} A_x\right)^2 - \left(\bar{p}_y - \frac{q}{p^o} A_y\right)^2} - \frac{q}{p^o l} A_z, \quad (12)$$

where

$$\mathbf{A} = \mathbf{A}(l\bar{x}, l\bar{y}, l\bar{t}/c; z), \quad \psi = \psi(l\bar{x}, l\bar{y}, l\bar{t}/c; z). \quad (13)$$

Lastly, go to the design trajectory by setting

$$\begin{aligned} X &= \bar{x}, & P_x &= \bar{p}_x, \\ Y &= \bar{y}, & P_y &= \bar{p}_y, \\ T &= \bar{t} - \bar{t}^g, & P_t &= \bar{p}_t - \bar{p}_t^g, \end{aligned} \quad (14)$$

where the superscript  $g$  denotes the “given” or “design” trajectory. We obtain a new Hamiltonian given by

$$H(X, P_x, Y, P_y, T, P_t; z) = -\frac{1}{l} \sqrt{\left(P_t + \bar{p}_t^g + \frac{q\psi}{p^o c}\right)^2 - \left(\frac{mc}{p^o}\right)^2 - \left(P_x - \frac{q}{p^o} A_x\right)^2 - \left(P_y - \frac{q}{p^o} A_y\right)^2} - \frac{q}{p^o l} A_z - \frac{\partial \bar{t}^g}{\partial z} P_t + \frac{\partial \bar{p}_t^g}{\partial z} T, \quad (15)$$

where

$$\mathbf{A} = \mathbf{A}\left(lX, lY, \frac{l}{c}(T + \bar{t}^g); z\right), \quad \psi = \psi\left(lX, lY, \frac{l}{c}(T + \bar{t}^g); z\right). \quad (16)$$

So far, we have been treating the full three-dimensional problem (in six-dimensional phase space). Now we will restrict ourselves to the two-dimensional (transverse beam dynamics) problem. To do this, we have to make certain assumptions about the longitudinal variables. First assume that, as particles propagate along the beam transport system, their total energy,  $-P_t$ , is constant or approximately constant. Since  $dP_t/dz = -\partial H/\partial T$ , this assumption is equivalent to the statement that all the fields (applied and self) are time-independent or weakly dependent on time. In fact, we will assume that all particles have the design energy, so that

$$P_t = 0. \quad (17)$$

Our calculation is greatly simplified if we neglect the longitudinal self-field,  $E_z$ . First, since we are using  $z$  as the independent variable, the transfer map has explicit  $x$ - and  $y$ -dependence, while the  $z$ -dependence is contained *implicitly* in the coefficients of  $\mathcal{M}$ . It is straightforward (though tedious) to obtain an approximate expression for the scalar potential in two dimensions (by solving Eq. (7) as a power series in  $x$  and  $y$ ). However, it would be difficult to solve the three-dimensional Poisson equation, because the  $z$ -dependence of the charge density would be contained implicitly in coefficients of  $\mathcal{M}$ . Second, the presence of a longitudinal self-field would make  $\bar{p}_t^g$  and unknown function of  $z$ , further complicating the problem. Thus, we will neglect the longitudinal self-field, as is often done in two-dimensional treatments of space charge. (An analysis that includes three-dimensional effects would be a worthwhile research project.)

Now consider a particle traveling along the axis of the beam transport system. Assuming there is no longitudinal electric field, no work can be done on the particle, so its kinetic energy must be constant. Since its total energy is also constant, it follows that the scalar potential on axis is a constant. We will arbitrarily set the scalar potential on axis equal to zero. (In general, the kinetic energy of a particle traveling along the axis and the potential on axis will vary with  $z$  as the beam size varies; however, if the space charge potential depression is small compared with the beam kinetic energy, then the potential on axis will be a *small*,  $z$ -dependent function. Our assumption is that this small  $z$ -dependent quantity can be neglected.) Summarizing, we will assume that a particle traveling along the axis has a constant kinetic energy and a constant value of  $p_z$  equal to the design value,  $p_z^g$ . Let the scale momentum,  $p^o$ , equal this design value,

$$p^o = \gamma^o m v^o = p_z^g. \quad (18)$$

For simplicity, we will take  $l = 1$  meter. Lastly, we will abuse notation and write  $(x, p_x, y, p_y)$  in place of  $(X, P_x, Y, P_y)$ .

Based on the previous discussion, the Hamiltonian becomes

$$H(x, p_x, y, p_y; z) = -\sqrt{1 - \frac{2q\psi}{p^0 v^0} + \left(\frac{q\psi}{p^0 c}\right)^2 - \left(p_x - \frac{q}{p^0} A_x\right)^2 - \left(p_y - \frac{q}{p^0} A_y\right)^2} - \frac{q}{p^0} A_z, \quad (19)$$

where

$$\mathbf{A} = \mathbf{A}(x, y; z), \quad \psi = \psi(x, y; z). \quad (20)$$

Here we have used the relations

$$(\bar{p}_i^g)^2 - \left(\frac{mc}{p^0}\right)^2 = 1 \quad (21)$$

and

$$\bar{p}_i^g/c = -\frac{1}{v^0}. \quad (22)$$

Now consider transport in a system consisting of drifts and solenoids. These applied fields can be represented (through third order) by a vector potential of the form shown below:

$$\begin{aligned} A_x &= -y \left[ \frac{1}{2} B(z, 0) - \frac{r^2}{16} B''(z, 0) \right], \\ A_y &= x \left[ \frac{1}{2} B(z, 0) - \frac{r^2}{16} B''(z, 0) \right], \\ A_z &= 0, \end{aligned} \quad (23)$$

where  $B(z, 0)$  is the longitudinal magnetic field at  $r = 0$ , and where a prime denotes differentiation with respect to  $z$ . Suppose the potentials associated with the self fields are given by

$$\begin{aligned} \psi &= \psi_2 r^2 + \psi_4 r^4, \\ A_x &= A_y = 0, \\ A_z &= \frac{v^0}{c^2} \psi. \end{aligned} \quad (24)$$

Note that we are neglecting the longitudinal self-magnetic field associated with  $v_\theta$ . (We are also neglecting the variation of  $v_z$  with radius in the calculation of the self vector potential,  $A_z$ .) It follows that the Hamiltonian is given by

$$H(x, p_x, y, p_y; z) = -\sqrt{1 + s_2 + s_4} - \frac{qv^0}{p^0 c^2} (\psi_2 r^2 + \psi_4 r^4), \quad (25)$$

where

$$s_2 = -p^2 - \alpha^2 r^2 + 2\alpha J_z - \frac{2q\psi_2}{p^0 v^0} r^2,$$

$$s_4 = \frac{\alpha\alpha''}{4} r^4 - \frac{\alpha''}{4} r^2 J_z + \left(\frac{q\psi_2}{p^0 c} r^2\right)^2 - \frac{2q\psi_4}{p^0 v^0} r^4, \quad (26)$$

and where

$$r^2 = x^2 + y^2,$$

$$p^2 = p_x^2 + p_y^2, \quad (27)$$

$$J_z = (\mathbf{r} \times \mathbf{p})_z = xp_y - yp_x.$$

The quantity  $\alpha(z)$  is proportional to the magnetic field on axis,

$$\alpha(z) = \frac{qB(z, 0)}{2p^0}. \quad (28)$$

Expanding the Hamiltonian we obtain

$$H = H_2 + H_4 + \dots, \quad (29)$$

where

$$H_2 = \frac{p^2}{2} + \frac{\alpha^2 r^2}{2} + \frac{q\psi_2 r^2}{p^0 v^0 (\gamma^0)^2} - \alpha J_z, \quad (30)$$

$$H_4 = \frac{(p^2)^2}{8} + \frac{\alpha^4 - \alpha\alpha''}{8} (r^2)^2 + \frac{3\alpha^2}{4} r^2 p^2 - \frac{\alpha^2}{2} (r \cdot p)^2 + \frac{\alpha'' - 4\alpha^3}{8} r^2 J_z - \frac{\alpha}{2} p^2 J_z$$

$$+ \left[ \frac{1}{2} \left( \frac{q\psi_2}{p^0 v^0 \gamma^0} \right)^2 + \frac{q\psi_4}{p^0 v^0 (\gamma^0)^2} + \frac{\alpha^2}{2} \left( \frac{q\psi_2}{p^0 v^0} \right) \right] (r^2)^2 + \frac{1}{2} \left( \frac{q\psi_2}{p^0 v^0} \right) r^2 p^2 - \alpha \left( \frac{q\psi_2}{p^0 v^0} \right) r^2 J_z. \quad (31)$$

Next introduce the notation

$$\psi_2 = \frac{\lambda_q}{4\pi\epsilon_0} \phi_2,$$

$$\psi_4 = \frac{\lambda_q}{4\pi\epsilon_0} \phi_4, \quad (32)$$

where, as mentioned previously,  $\lambda_q$  is the line charge density. Following tradition, we will let  $K$  denote the generalized perveance<sup>8</sup>:

$$K = \frac{2q\lambda_q}{4\pi\epsilon_0 p^0 v^0 (\gamma^0)^2}. \quad (33)$$



Finally, we obtain

$$H_2 = \frac{p^2}{2} + \frac{\alpha^2 r^2}{2} + \frac{K\phi_2}{2} r^2 - \alpha J_z, \quad (34)$$

$$\begin{aligned} H_4 = & \frac{(p^2)^2}{8} + \frac{\alpha^4 - \alpha\alpha''}{8} (r^2)^2 + \frac{3\alpha^2}{4} r^2 p^2 - \frac{\alpha^2}{2} (r \cdot p)^2 + \frac{\alpha'' - 4\alpha^3}{8} r^2 J_z - \frac{\alpha}{2} p^2 J_z \\ & + \left[ \frac{1}{8} (\gamma^0 K \phi_2)^2 + \frac{1}{2} K \phi_4 + \frac{\alpha^2}{2} (\gamma^0)^2 K \phi_2 \right] (r^2)^2 \\ & + \frac{(\gamma^0)^2 K \phi_2}{4} r^2 p^2 - \frac{\alpha(\gamma^0)^2 K \phi_2}{2} r^2 J_z. \end{aligned} \quad (35)$$

For future reference, we shall write  $H_2 = H_2^O + H_2^R$ , where

$$\begin{aligned} H_2^O &= \frac{p^2}{2} + \frac{\alpha^2 r^2}{2} + \frac{K\phi_2 r^2}{2}, \\ H_2^R &= -\alpha J_z. \end{aligned} \quad (36)$$

Note that  $H_2^O$  governs the optical behavior of the map (in the paraxial approximation) and  $H_2^R$  simply generates rotations about the optical axis. Finally, note that when  $\phi_2 = \phi_4 = 0$ , these results agree with the standard results for a solenoid.<sup>9,10,11</sup>

## 5 OVERVIEW OF LIE ALGEBRAIC TOOLS

Consider an  $m$ -dimensional dynamical system governed by some Hamiltonian  $H(\zeta, t)$ , where  $\zeta = (q_1, p_1, q_2, p_2, \dots, q_m, p_m)$ . (For our two-dimensional problem,  $\zeta = (x, p_x, y, p_y)$ , and the independent variable “ $t$ ” is really the longitudinal coordinate  $z$ .) The evolution of the system is governed by Hamilton’s equations,

$$\begin{aligned} \frac{dq_i}{dt} &= \frac{\partial H}{\partial p_i}, \\ \frac{dp_i}{dt} &= -\frac{\partial H}{\partial q_i}. \end{aligned} \quad (37)$$

As mentioned earlier, we can associate a (generally nonlinear) mapping,  $\mathcal{M}$ , with this system. Now, since  $\mathcal{M}$  is related to the above equations, it cannot have just any form; maps that are derived from Hamiltonian systems belong to a class of mappings called *symplectic* mappings. Since our goal is to calculate a map for a Hamiltonian system, it makes sense to choose a representation of  $\mathcal{M}$  that is manifestly symplectic. This is where Lie algebraic tools come into play.

We will not give a detailed exposition of Lie algebraic tools here. The application of Lie algebraic tools to problems in accelerator physics is described in the literature.<sup>12,13</sup> Instead, we will provide a brief review of the results that are relevant to this report.

Before we can state the Lie algebraic representation of  $\mathcal{M}$  we need to define certain quantities. First, let  $f$  denote any function of  $(\mathbf{q}, \mathbf{p})$  and  $t$ . The *Lie operator* associated with  $f$ , which we shall denote  $:f:$ , is defined by the rule

$$:f:g = [f, g], \tag{38}$$

where  $g$  is also any function of  $(\mathbf{q}, \mathbf{p})$  and  $t$ , and where  $[, ]$  denotes the Poisson bracket,

$$[f, g] = \sum_i \left( \frac{\partial f}{\partial q_i} \frac{\partial g}{\partial p_i} - \frac{\partial f}{\partial p_i} \frac{\partial g}{\partial q_i} \right). \tag{39}$$

The *Lie transformation* associated with  $f$  is the operator that is the exponential of  $:f:$ ,

$$e^{:f:} = \sum_{n=0}^{\infty} \frac{:f:^n}{n!}. \tag{40}$$

As shown above, the Lie transformation is defined formally in terms of the power series expansion of the exponential function. In the above expression, powers of  $:f:$  are defined according to

$$\begin{aligned} :f:^0 g &= g, \\ :f:^1 g &= [f, g], \\ :f:^2 g &= [f, [f, g]], \\ &\vdots \end{aligned} \tag{41}$$

Now we are ready to define the Lie algebraic representation of  $\mathcal{M}$ . The Lie algebraic representation of  $\mathcal{M}$  is given by

$$\mathcal{M} = e^{:f_2:} e^{:f_3:} e^{:f_4:} \dots \tag{42}$$

That is,  $\mathcal{M}$  is represented as an infinite product of Lie transformations. The quantities  $:f_n:$  are homogeneous polynomials of degree  $n$  in  $\mathbf{q}$  and  $\mathbf{p}$ . (For example, in one dimension the polynomial  $:f_2:$  is of the form  $aq^2 + bqp + cp^2$ ). This representation has certain important features:

- 1) The quantity  $e^{:f_2:}$  is a linear mapping. That is, there exists a matrix  $M$  such that

$$e^{:f_2:} \zeta = M \zeta. \tag{43}$$

- 2) The polynomials  $f_3, f_4, \dots$  describe nonlinear effects. For example,  $f_3$  is related to second-order effects and  $f_4$  is related to third-order effects.

- 3) The polynomials  $f_3, f_4, \dots$  utilize the *minimum* number of coefficients to specify  $\mathcal{M}$  to a given order.

A third order representation of  $\mathcal{M}$  is given by the truncated product

$$\mathcal{M} = e^{:f_2:} e^{:f_3:} e^{:f_4:}. \tag{44}$$

By expanding the exponentials associated with  $f_3$  and  $f_4$ , dropping terms beyond third order (in  $\zeta$ ), we obtain

$$\mathcal{M} = e^{i f_3} [1 + : f_3 : + (\frac{1}{2} : f_3 :^2 + : f_4 :)]. \quad (45)$$

In particular, we are interested in the action of  $\mathcal{M}$  on each component of  $\zeta$ :

$$\mathcal{M} \zeta_a = e^{i f_2} \zeta_a + e^{i f_2} : f_3 : \zeta_a + e^{i f_2} (\frac{1}{2} : f_3 :^2 + : f_4 :) \zeta_a. \quad (46)$$

It is easy to show that the terms in the above Lie series are related to corresponding terms in the usual Taylor series representation. The relationship between the two series (for an  $m$ -dimensional system) is shown below:

$$\begin{aligned} \zeta_a^f &= \sum_{b=1}^{2m} M_{ab} \zeta_b^i + \sum_{1 \leq b \leq c}^{2m} T_{abc} \zeta_b^i \zeta_c^i + \sum_{1 \leq b \leq c \leq d}^{2m} U_{abcd} \zeta_b^i \zeta_c^i \zeta_d^i + \dots \\ &\quad \Downarrow \qquad \qquad \Downarrow \qquad \qquad \Downarrow \\ \zeta_a^f &= e^{i f_2} \zeta_a^i + e^{i f_2} : f_3 : \zeta_a^i + e^{i f_2} (\frac{1}{2} : f_3 :^2 + : f_4 :) \zeta_a^i + \dots \end{aligned} \quad (47)$$

Although, due to our expanding the exponentials in equation (44), the transformation (46) is not symplectic, it still uses fewer parameters than the conventional Taylor series approach because we started out using a Lie algebraic representation.

A further advantage of the Lie algebraic approach is that the equations of motion for  $\mathcal{M}$  can be expressed as a simple standard set of differential equations.<sup>14</sup> In this case, let  $\mathcal{M}$  be represented in the following form:

$$\mathcal{M} = \dots e^{i g_4} e^{i g_3} e^{i g_2}, \quad (48)$$

where, as before, each  $g_n$  is a homogeneous polynomial of degree  $n$  in  $\zeta$ . Suppose the Hamiltonian is expanded in a power series around the design orbit:

$$H = H_2 + H_3 + H_4 \dots \quad (49)$$

It can be shown that the linear transfer matrix,  $M$  (corresponding to  $e^{i g_2}$ ) obeys the differential equation

$$M' = JSM, \quad (50)$$

where  $S$  is a symmetric matrix defined in terms of the quadratic part of the Hamiltonian,

$$H_2 = \frac{1}{2} \sum_{a,b=1}^{2m} S_{ab} \zeta_a \zeta_b, \quad (51)$$

and where the matrix elements of  $J$  are given by

$$J_{ab} = [\zeta_a, \zeta_b]. \quad (52)$$

Here a prime denotes differentiation with respect to the independent variable (which is the longitudinal coordinate,  $z$ , in our case). Also, it can be shown that  $g_3$  and  $g_4$  obey the equations

$$\begin{aligned} g_3' &= -H_3^{\text{int}}, \\ g_4' &= -H_4^{\text{int}} + \frac{1}{2} : f_3 : (-H_3^{\text{int}}), \end{aligned} \quad (53)$$

where the interaction Hamiltonian is defined according to

$$H_n^{\text{int}} = H_n(M\zeta). \quad (54)$$

That is,  $H_n^{\text{int}}$  is obtained from  $H_n$  by transforming its arguments with the matrix  $M$ . (Note that, since  $M$  is  $z$ -dependent,  $H_n^{\text{int}}$  will also be  $z$ -dependent even though  $H_n$  may be independent of  $z$ ).

To close this section, we wish to clarify our reasons for using a Lie algebraic representation of  $\mathcal{M}$ . First it is worth pointing out that, though maintaining the symplectic condition is crucial for calculating long term behavior in periodic beam transport systems, it is not crucial to the present calculation; our results are valid for short, one-pass systems that can be represented by a single mapping. (See the discussion in section 10.) Besides, the transformation (46) is not symplectic anyway. Why, then, did we use a Lie algebraic approach? We did so because the purpose of the present calculation is to obtain a mapping, and it makes sense to use whatever tools make this as easy as possible. As mentioned earlier, the Lie algebraic representation utilizes the minimum number of parameters to specify a map to a given order; this greatly simplifies the calculation of the self-consistent scalar potential given in Appendix A. Furthermore, the equations of motion for  $\mathcal{M}$  are given by the simple set of ordinary differential equations shown above. This calculation could of course have been done using a Taylor series representation, but it would have made the calculation far more tedious.

In the next section we will derive the equations for  $M$  and  $g_4$  corresponding to an axisymmetric beam with space charge propagating through drifts and magnetic solenoids.

## 6 THE EQUATIONS OF MOTION FOR $\mathcal{M}$

Since the Hamiltonian (29) contains no third-order terms, a third-order representation of  $\mathcal{M}$  is given by

$$\mathcal{M} = e^{:g_4:} e^{:g_2:}. \quad (55)$$

Since the operators  $:H_2^O:$  and  $:H_2^R:$  commute with each other (that is, their Poisson bracket is zero), the mapping  $\mathcal{M}_2$  can be written as a product of commuting maps of the form

$$\mathcal{M}_2 = \mathcal{M}_2^R \mathcal{M}_2^O. \quad (56)$$

It follows that the matrix representation of  $\mathcal{M}_2$ , which we shall denote  $M$ , is given by

$$M = M^O R, \quad (57)$$

where

$$M^O = \begin{pmatrix} a & b & 0 & 0 \\ c & d & 0 & 0 \\ 0 & 0 & a & b \\ 0 & 0 & c & d \end{pmatrix}, \quad (58)$$

where  $R$  is a rotation matrix,

$$R = \begin{pmatrix} \cos \theta & 0 & \sin \theta & \theta \\ 0 & \cos \theta & 0 & \sin \theta \\ -\sin \theta & 0 & \cos \theta & 0 \\ 0 & -\sin \theta & 0 & \cos \theta \end{pmatrix}, \quad (59)$$

and where

$$\theta = \int_{z^i}^{z^f} \alpha(z) dz. \quad (60)$$

Since we are dealing with systems having cylindrical symmetry,  $R$  will play no role in the calculation of the scalar potential. By analogy with the results of the previous section, it is possible to show that  $M^O$  satisfies the following equation:

$$\frac{dM^O}{dz} = JSM^O, \quad (61)$$

where

$$S = \begin{pmatrix} \alpha^2 + K\phi_2 & 0 & 0 & 0 \\ 0 & 1 & 0 & 0 \\ 0 & 0 & \alpha^2 + K\phi_2 & 0 \\ 0 & 0 & 0 & 1 \end{pmatrix}, \quad (62)$$

It follows that the matrix elements of  $M^O$  satisfy the following differential equations,

$$\begin{aligned} a' &= c, \\ b' &= d, \\ c' &= -(\alpha^2 + K\phi_2)a, \\ d' &= -(\alpha^2 + K\phi_2)b, \end{aligned} \quad (63)$$

where a prime denotes  $d/dz$ , and with the initial condition  $M^O(z^i) = I$  (the identity matrix). These equations can be expressed as two second order equations,

$$\begin{aligned} a'' + (\alpha^2 + K\phi_2)a &= 0, \\ b'' + (\alpha^2 + K\phi_2)b &= 0. \end{aligned} \quad (64)$$

Next, it follows from symmetry that  $g_4$  is of the form

$$\begin{aligned} g_4 &= e_1(p^2)^2 + e_2p^2(r \cdot p) + e_3p^2(r \times p)_z + e_4(r \cdot p)^2 + e_5(r \cdot p)(r \times p)_z \\ &+ e_6r^2p^2 + e_7r^2(r \cdot p) + e_8r^2(r \times p)_z + e_9(r^2)^2. \end{aligned} \quad (65)$$

Using Eq. (53) (with  $H_3^{\text{int}} = 0$ ), we obtain the following differential equations for the coefficients  $e_1$  through  $e_9$ :

$$\frac{de_1}{dz} = \frac{b^4}{8}(\alpha\alpha'' + \delta) - \frac{1}{8}((b')^2 + b^2\hat{\alpha}^2)^2, \quad (66a)$$

$$\frac{de_2}{dz} = \frac{ab^3}{2}(\alpha\alpha'' + \delta) - \frac{1}{2}((b')^2 + b^2\hat{\alpha}^2)(a'b' + ab\hat{\alpha}^2), \quad (66b)$$

$$\frac{de_3}{dz} = \frac{\alpha}{2}((b')^2 + b^2\hat{\alpha}^2) - \frac{\alpha''b^2}{8}, \quad (66c)$$

$$\frac{de_4}{dz} = \frac{1}{2}\{\alpha^2 + a^2b^2(\alpha\alpha'' + \delta) - (a'b' + ab\hat{\alpha}^2)^2\}, \quad (66d)$$

$$\frac{de_5}{dz} = \alpha(a'b' + ab\hat{\alpha}^2) - \frac{\alpha''ab}{4}, \quad (66e)$$

$$\frac{de_6}{dz} = \frac{a^2b^2}{4}(\alpha\alpha'' + \delta) - \frac{\alpha^2}{2} - \frac{1}{4}((a')^2 + a^2\hat{\alpha}^2)((b')^2 + b^2\hat{\alpha}^2), \quad (66f)$$

$$\frac{de_7}{dz} = \frac{a^3b}{2}(\alpha\alpha'' + \delta) - \frac{1}{2}((a')^2 + a^2\hat{\alpha}^2)(a'b' + ab\hat{\alpha}^2), \quad (66g)$$

$$\frac{de_8}{dz} = \frac{\alpha}{2}((a')^2 + a^2\hat{\alpha}^2) - \frac{\alpha''a^2}{8}, \quad (66h)$$

$$\frac{de_9}{dz} = \frac{a^4}{8}(\alpha\alpha'' + \delta) - \frac{1}{8}((a')^2 + a^2\hat{\alpha}^2)^2. \quad (66i)$$

In the above equations, the quantities  $\hat{\alpha}^2$  and  $\delta$  are given by

$$\begin{aligned} \hat{\alpha}^2 &= \alpha^2 + (\gamma^0)^2 K\phi_2, \\ \delta &= ((\gamma^0)^2 \beta^0 K\phi_2)^2 - 4K\phi_4. \end{aligned} \quad (67)$$

Summarizing, we have derived equations for the 13 quantities  $a$ ,  $b$ ,  $c$ ,  $d$  and  $e_1$  through  $e_9$  that characterize  $\mathcal{M}$  through third order. Now all that remains is to calculate the quantities  $\phi_2$  and  $\phi_4$ , which are themselves functions of  $a$ ,  $b$ ,  $c$ ,  $d$  and  $e_1$  through  $e_9$ . This is the subject of the next section.

## 7 CALCULATION OF THE SCALAR POTENTIAL

Consider a beam characterized by an initial distribution function of the form

$$f^o(\zeta) = \frac{1}{2\pi\lambda^2} e^{-(p_x^2 + p_y^2)/2\lambda^2} \rho^o(x^2 + y^2), \quad (68)$$

where

$$\iint dx dy \rho^o = 1. \quad (69)$$

The  $z$ -dependent distribution function is given by

$$f(\zeta; z) = f^o(\mathcal{M}^{-1}\zeta), \quad (70)$$

where  $\mathcal{M}$  is the map between  $z^i$  and  $z^f$ .

Now, formally, the scalar potential is given by

$$\psi(x, y; z) = \frac{\lambda_a}{(2\pi)^2 \varepsilon_0} \int d^4 \zeta' \int d^2 k \frac{1}{k^2} e^{ik_x(x-x')} e^{ik_y(y-y')} f^o(\mathcal{M}^{-1} \zeta'). \quad (71)$$

After a very tedious calculation (performed with the help of MATHEMATICA<sup>15</sup>), we obtain

$$\psi = \frac{\lambda_a}{4\pi \varepsilon_0} (\phi_2 r^2 + \phi_4 r^4 + \dots), \quad (72)$$

where

$$\begin{aligned} -2a^3 \phi_2 &= [a^3 + 8\lambda^2(a^3 e_2 - 2a^2 b(e_4 + e_6) + 3ab^2 e_7 - 4b^3 e_9)] R\left(\frac{\lambda^2 b^2}{2}\right) \\ &+ 4\lambda^4 b[-4a^4 e_1 + 5a^3 b e_2 - 6a^2 b^2(e_4 + e_6) + 7ab^3 e_7 - 8b^4 e_9] R'\left(\frac{\lambda^2 b^2}{2}\right) \\ &+ 4\lambda^6 b^3[-a^4 e_1 + a^3 b e_2 - a^2 b^2(e_4 + e_6) + ab^3 e_7 - b^4 e_9] R''\left(\frac{\lambda^2 b^2}{2}\right), \quad (73) \\ -32a^3 \phi_4 &= 16(ae_7 - 4be_9) R\left(\frac{\lambda^2 b^2}{2}\right) \\ &+ [a^3 + 16\lambda^2(a^3 e_2 - 3a^2 b(e_4 + e_6) + 6ab^2 e_7 - 10b^3 e_9)] R'\left(\frac{\lambda^2 b^2}{2}\right) \\ &+ 2\lambda^4 b[-8a^4 e_1 + 13a^3 b e_2 - 18a^2 b^2(e_4 + e_6) \\ &+ 23ab^3 e_7 - 28b^4 e_9] R''\left(\frac{\lambda^2 b^2}{2}\right) \\ &+ 4\lambda^6 b^3[-a^4 e_1 + a^3 b e_2 - a^2 b^2(e_4 + e_6) + ab^3 e_7 - b^4 e_9] R'''\left(\frac{\lambda^2 b^2}{2}\right). \quad (74) \end{aligned}$$

(The details of this calculation are given in an appendix.) In the above equations, the quantity  $R(u)$  is a quantity that depends on the initial density and is given by

$$R(u) = 2\pi \int_0^\infty dk k e^{-uk^2} \int_0^\infty dr r J_0(akr) \rho^o(r) = \frac{\pi}{u} \int_0^\infty dr r \rho^o(r) e^{-a^2 r^2 / 4u}. \quad (75)$$

Note that for an initially uniform beam,

$$\rho^o(r) = \frac{1}{\pi \sigma^2} \begin{cases} 1 & \text{if } r \leq \sigma \\ 0 & \text{elsewhere} \end{cases}, \quad (76)$$

and  $R(u)$  is given by

$$R(u) = \frac{2}{a^2 \sigma^2} \left(1 - e^{-a^2 \sigma^2 / 4u}\right). \quad (77)$$

The above formulas for  $\phi_2$  and  $\phi_4$  depend on the quantity  $R(\lambda^2 b^2/2)$ ; for an initially uniform beam,

$$R(\lambda^2 b^2/2) = \frac{2}{a^2 \sigma^2} (1 - e^{-a^2 \sigma^2 / 2 \lambda^2 b^2}). \quad (78)$$

Substitution of Eqs. (73) and (74) into Eqs. (64) and (66) yields a closed set of differential equations for a third-order representation of  $\mathcal{M}$ .

## 8 THE COMPUTER PROGRAM *SOLMAP*

The equations (64) for the evolution of  $M^O$  and (66) for the evolution of  $g_4$ , (along with Eqs. (73) and (74) for the self-consistent scalar potential) constitute a set of 13 coupled ordinary differential equations for the self-consistent transfer map. These have been coded into a FORTRAN77 program called *SOLMAP*. The program computes the solenoid map with space charge through 3rd order, assuming the initial distribution function is given by

$$f^o(\zeta) = \frac{1}{2\pi\lambda^2} e^{-(p_x^2 + p_y^2)/2\lambda^2} \rho^o(x^2 + y^2). \quad (79)$$

That is, the initial distribution function is assumed to be the product of a Gaussian in momentum space times a function of  $r$ . Depending on the choice of  $\rho^o$ , the user must specify  $R(u)$  (see Eq. (75)) and its first three derivatives in statement functions.

The result of running *SOLMAP* is a transfer map in the form (55). (That is, *SOLMAP* computes the matrix elements of  $M^O$  and the 9 coefficients of the polynomial  $g_4$ .) This map can be used by a Lie algebraic beam transport code, such as *MARYLIE* 3.0, to propagate particles. (We will show an example of this in the next section.) Alternatively, the map can be converted to the form of Eq. (5) and used by other transfer map codes, such as *TRANSPORT* and *MAD*.

We have written *SOLMAP* so that it can be easily incorporated as a subroutine in *MARYLIE*. This makes it possible to utilize the powerful fitting and optimization routines of *MARYLIE* to design magnetic optics systems in the presence of space charge. We hope to perform this work in the future.

The next section contains a comparison of *SOLMAP* with particle simulation for a simple magnetic optics system.

## 9 NONLINEAR EFFECTS ASSOCIATED WITH FOCUSING BY A SOLENOID LENS

The example we will consider is based on a beam transport experiment performed by P. Loschialpo<sup>16</sup>. In this experiment, an electron beam is produced by a Pierce-type gun with a shielded cathode. The particles pass through a fine mesh in the gun anode and travel downstream where they are focused by a solenoid. The density profile of



e beam:  $r(0) = 5 \text{ mm}$   
 $I = 78 \text{ ma}$   
 $E = 5 \text{ keV}$

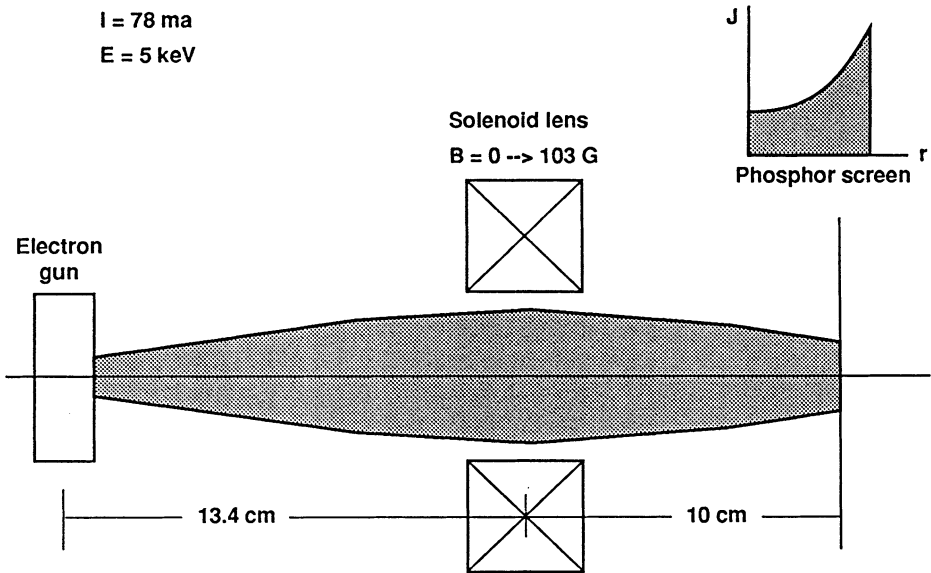


FIGURE 1 Configuration of an experiment to study nonlinear optical effects and nonlinear space charge effects associated with the focusing of an electron beam by a solenoid.

the electron beam is measured downstream of the solenoid for several values of (peak) magnetic field. See Figure 1. The parameters of the experiment are chosen so that both lens aberrations and space charge effects are important. The axial magnetic field is given approximately by

$$B(0, z) = \frac{B_0 e^{-z^2/2b^2}}{1 + z^2/a^2}, \quad (80)$$

where  $a = 4.40 \text{ cm}$  and  $b = 2.29 \text{ cm}$ .

In our example the magnet center is located at  $z = 0$ . The beam is launched  $13.4 \text{ cm}$  upstream of the magnet center. The beam emitted from the gun is assumed to be a cold, uniform beam (though our analysis can include beams with thermal velocity distributions). The initial beam radius is  $5 \text{ mm}$ , the beam current is  $78 \text{ mA}$ , and the beam energy is  $5 \text{ keV}$ .

In our example, a numerical distribution of particles (cylindrical shells) was propagated through the solenoid in two ways:

1) The map  $\mathcal{M}$  was calculated using SOLMAP. (A cold beam is obtained from our formulas by taking the limit as  $\lambda$  tends to zero. To avoid numerical difficulties, we simply ran SOLMAP with  $\lambda = 1 \times 10^{-8}$ .) Then the map was applied to the initial distribution of particles using MARYLIE to produce the final distribution.

2) The final distribution was produced by running a particle simulation. The simulation is based on numerical integration of Hamilton's equations in cylindrical coordinates, and is discussed in an appendix.

The results of these two procedures were compared in several ways, as discussed below.

First we compared the beam current density as a function of  $r$ . This was done by first calculating a quantity  $F(r)$  equal to the number of particles inside a cylinder of radius  $r$ :

$$F(r_k) = \frac{1}{N} \sum_{r_k \leq r} 1. \quad (81)$$

The charge density can be obtained by numerically differentiating  $F(r)$ , since

$$\lambda_q F(r) = 2\pi \int_0^r r' \rho(r') dr', \quad (82)$$

from which we obtain

$$\rho(r) = \frac{\lambda_q}{2\pi r} \frac{dF}{dr}. \quad (83)$$

Neglecting the variation of  $v_z$  with radius, it follows that the longitudinal current density is given by

$$J(r) = \frac{I}{2\pi r} \frac{dF}{dr}. \quad (84)$$

We numerically differentiated  $F(r)$  using 5-point Lagrange interpolation for the derivative of a function<sup>17</sup>. Our results are shown in Figures 2 through 5. Figure 2

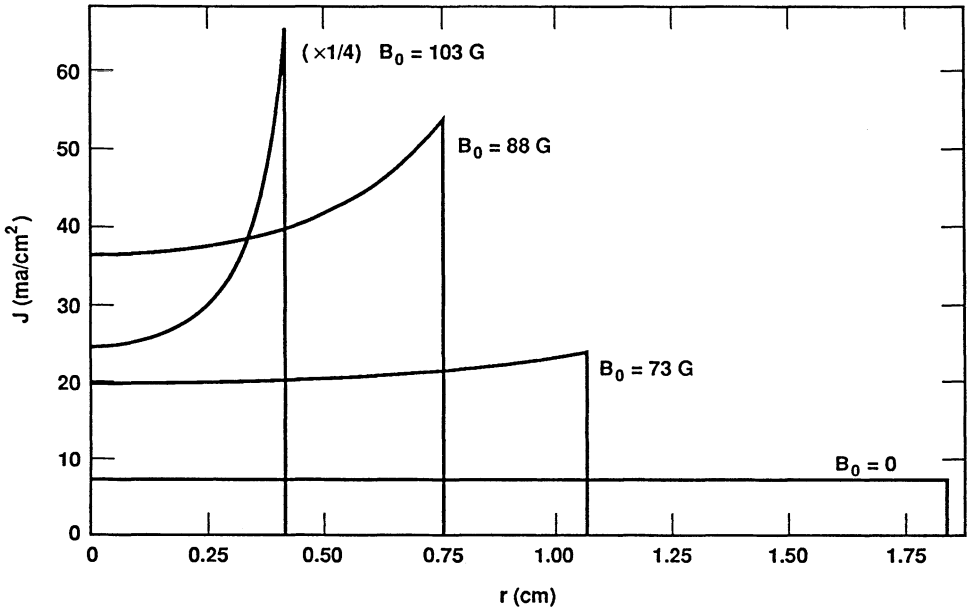


FIGURE 2 Current density profiles at  $z = 10$  cm with  $B_0 = 0$ ,  $B_0 = 73$  G,  $B_0 = 88$  G, and  $B_0 = 103$  G. The results are based on final particle coordinates obtained using SOLMAP and MARYLIE.

shows plots of the current density at  $z = 10$  cm for  $B_0 = 0$ ,  $B_0 = 73$  G,  $B_0 = 88$  G, and  $B_0 = 103$  G. For each value of  $B_0$ , the density was calculated using the final distribution from SOLMAP/MARYLIE. Note that the beam becomes quite hollow for increasing values of  $B_0$ . Next we computed the current density using the final distribution of particles from particle simulation, and we compared the results with the profiles obtained from SOLMAP/MARYLIE. Figures 3, 4 and 5 show the results for  $B_0 = 73$  G, 88 G and 103 G, respectively. (For  $B_0 = 0$ , the transfer map results and the simulation results are indistinguishable; in these simulations the initial distribution is cold and uniform, so there are no nonlinear forces in the problem when  $B_0 = 0$ .) It is clear that the results obtained using self-consistent transfer maps are in excellent agreement with simulation. Also, the results are in good agreement with the experimentally measured profiles obtained by P. Loschialpo.<sup>18</sup> Figure 6 is a plot of  $J(r)$  at  $z = 10$  cm for  $B_0 = 88$  G, but with the space charge forces omitted from the calculation. Comparing with Figure 4, it is clear that space charge forces are significant in this example.

Next we used our method to predict rms beam size and emittance growth, and we compared our results with simulation. Using transfer map methods, it is possible to compute the moments *directly* from the map, without using particles to perform rms sums. All that is required is the transfer map and some moments of the initial distribution function. For example, in one dimension, the expectation value of the quantity  $x^j p_x^k$  is given by

$$\langle x^j p_x^k \rangle(z) = \int dx dp_x f^o(x, p_x) (\mathcal{M}x)^j (\mathcal{M}p_x)^k. \quad (85)$$

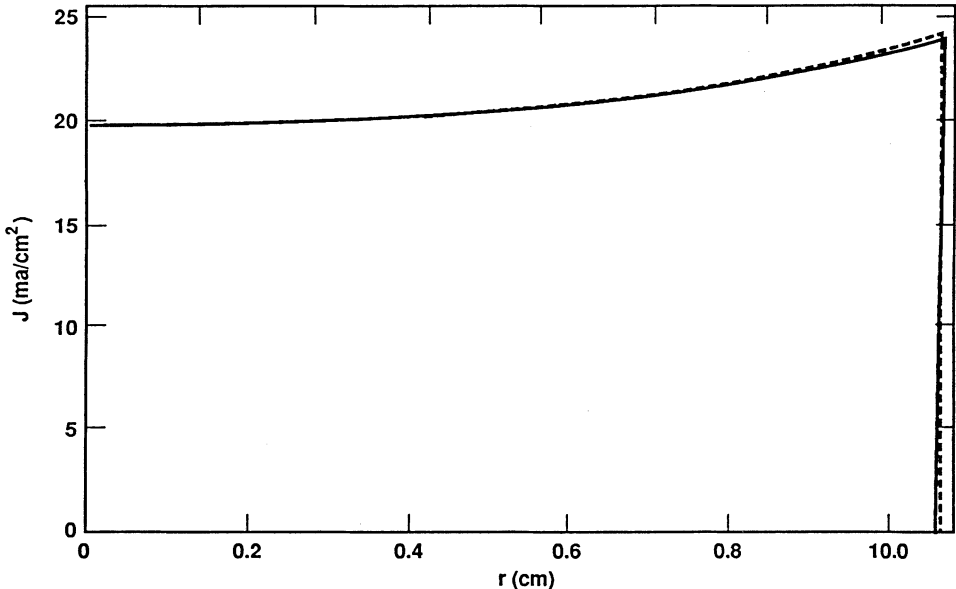


FIGURE 3 Current density profile at  $z = 10$  cm with  $B_0 = 73$  G. The solid curve was obtained using SOLMAP and MARYLIE. The dashed curve was obtained using a particle simulation.

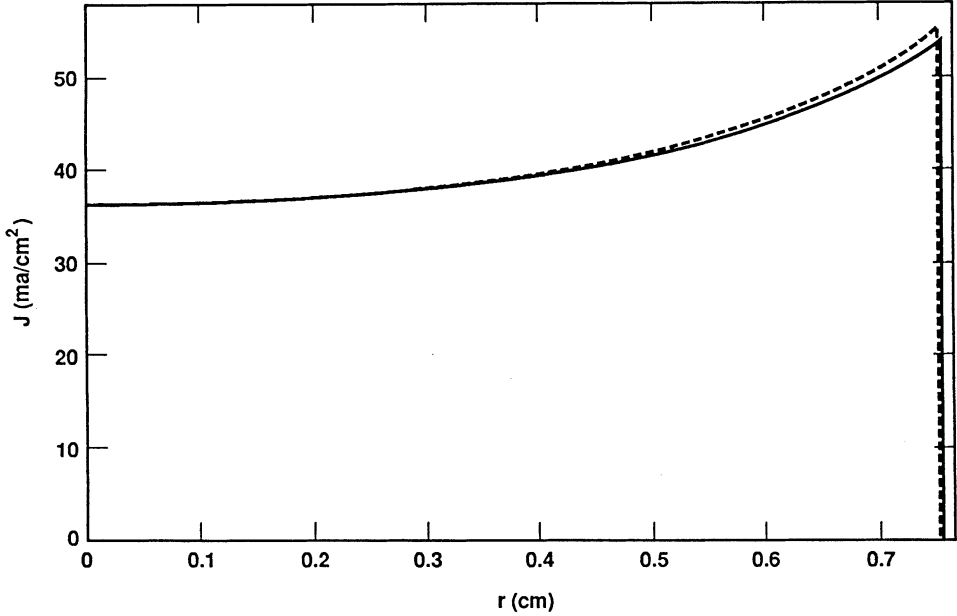


FIGURE 4 Current density profile at  $z = 10$  cm with  $B_0 = 88$  G. The solid curve was obtained using SOLMAP and MARYLIE. The dashed curve was obtained using a particle simulation.

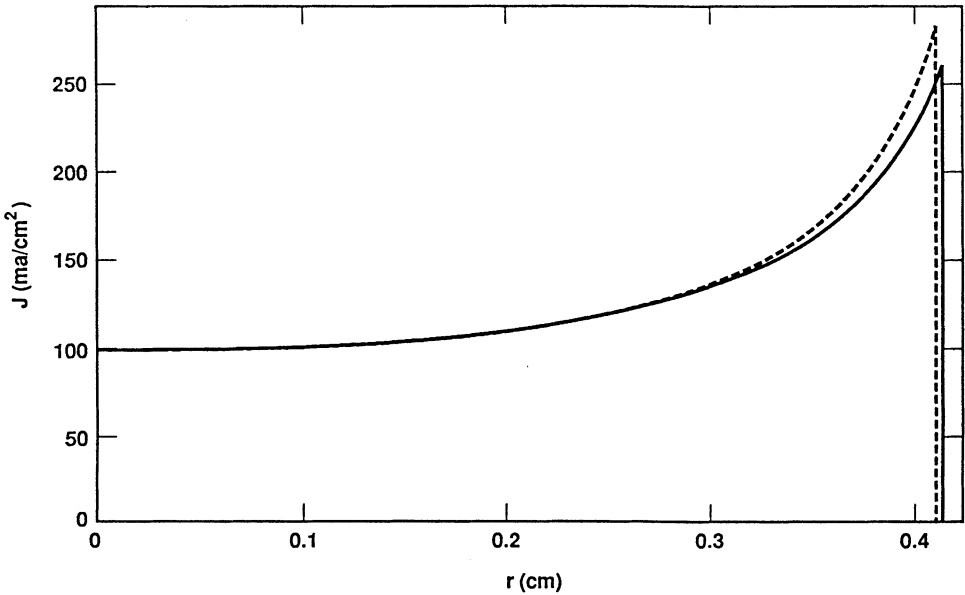


FIGURE 5 Current density profile at  $z = 10$  cm with  $B_0 = 103$  G. The solid curve was obtained using SOLMAP and MARYLIE. The dashed curve was obtained using a particle simulation.

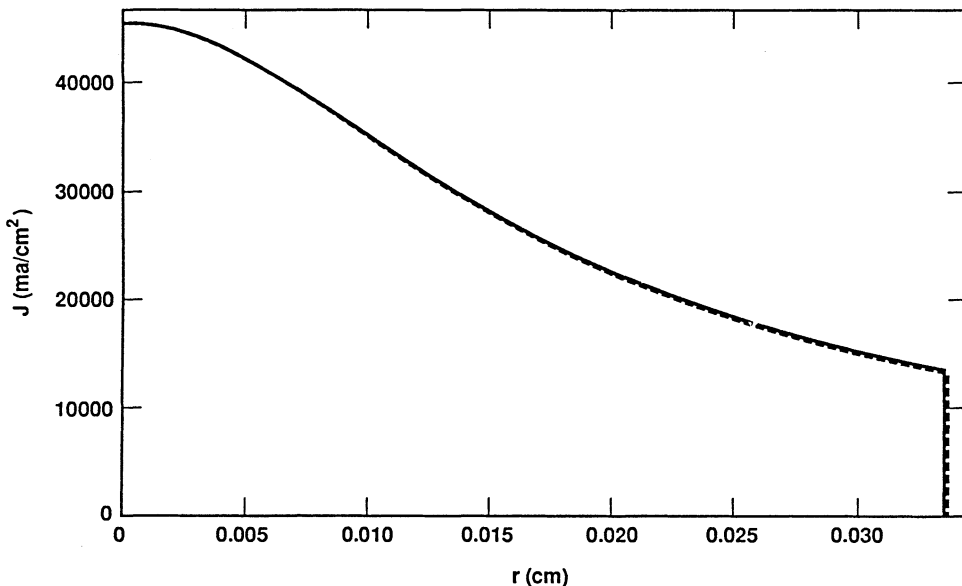


FIGURE 6 Current density profile at  $z = 10$  cm with  $B_0 = 88$  G. Space charge forces have been neglected. The solid curve was obtained using SOLMAP and MARYLIE. The dashed curve was obtained using a particle simulation.

By expanding  $\mathcal{M}$  inside the above integral, one obtains an equation for the final moment as a power series in the initial moments. For our problem it is easy to show that the final mean squared beam radius is related to the initial mean squared radius (through third order) according to:

$$\langle r^2 \rangle^f = a^2 \langle r^2 \rangle^i + 2a(4be_9 - ae_7) \langle r^4 \rangle^i + (4be_9 - ae_7)^2 \langle r^6 \rangle^i + \dots, \quad (86)$$

where  $a$ ,  $b$ ,  $e_7$  and  $e_9$  are coefficients of  $\mathcal{M}$ . (Note that the series contains no terms involving moments of  $p$  because the beam particles are all assumed to have  $p_x^i = p_y^i = 0$ .) Similar equations can be obtained for the quantities  $\langle r \cdot p \rangle = \langle xp_x + yp_y \rangle$  and  $\langle p^2 \rangle = \langle p_x^2 + p_y^2 \rangle$ :

$$\langle p^2 \rangle^f = c^2 \langle r^2 \rangle^i + 2c(4de_9 - ce_7) \langle r^4 \rangle^i + (4de_9 - ce_7)^2 \langle r^6 \rangle^i + \dots, \quad (87)$$

$$\begin{aligned} \langle r \cdot p \rangle^f = & ac \langle r^2 \rangle^i + [a(4de_9 - ce_7) + c(4be_9 - ae_7)] \langle r^4 \rangle^i \\ & + (4be_9 - ae_7)(4de_9 - ce_7) \langle r^6 \rangle^i + \dots. \end{aligned} \quad (88)$$

Lastly, these can be combined to produce a quantity  $\varepsilon^2$ , where

$$\varepsilon^2 = \langle r^2 \rangle \langle p^2 \rangle - (\langle r \cdot p \rangle)^2. \quad (89)$$

This is related to the mean square emittance, and it is highly sensitive to nonlinear effects.<sup>19</sup> Substituting the above formulas, we obtain

$$\varepsilon^2 = (4e_9)^2 [\langle r^2 \rangle^i \langle r^6 \rangle^i - \langle r^4 \rangle^i \langle r^4 \rangle^i] + \dots. \quad (90)$$

Thus, in this case the coefficient  $e_9$  governs the lowest-order emittance growth.

These moments can be calculated using particle simulation by performing the appropriate rms sums over the macroparticles, and compared with results obtained using SOLMAP along with the above formulas. Figure 7 is a plot of the root mean squared radius,  $\langle r^2 \rangle^{1/2}$ , as a function of distance using these two methods. (In this example,  $B_0 = 103$  G and the calculation is carried out to  $z = 16$  cm.) In this case the curves are so similar that they are nearly indistinguishable. The figure also shows the transfer map result with the nonlinear corrections omitted. It is clear that the nonlinear corrections are necessary in order to accurately compute the beam radius at the waist. Plots of  $\langle p^2 \rangle^{1/2}$  and  $\langle r \cdot p \rangle$  also show excellent agreement with simulation. For example, Figure 8 is a plot of  $\langle p^2 \rangle^{1/2}$  as a function of  $z$ . Figure 9 is a plot of  $\langle r^2 \rangle^{1/2}$  as a function of  $z$  with the space charge forces omitted. (In this figure,  $\langle r^2 \rangle^{1/2}$  has a minimum value of  $17 \mu\text{m}$  at  $z \approx 7$  cm.) Comparing with Figure 7, it is clear that space charge plays an important role in these simulations.

Lastly, Figure 10 is a plot of  $\varepsilon$  as a function of  $z$ . The curves are less similar than the curves for  $\langle r^2 \rangle^{1/2}$  and  $\langle p^2 \rangle^{1/2}$ , but there is still good agreement between the transfer map results and the simulation results.<sup>20</sup>

Summarizing, our method based on self-consistent transfer maps gives results that are in good agreement with particle simulation. However, the particle simulation required integration of several thousand trajectories (we used 2500 macroparticles in these examples), whereas our method required the integration of just  $4 + 9 = 13$  equations. If we had compared our method with particle simulation at larger distances

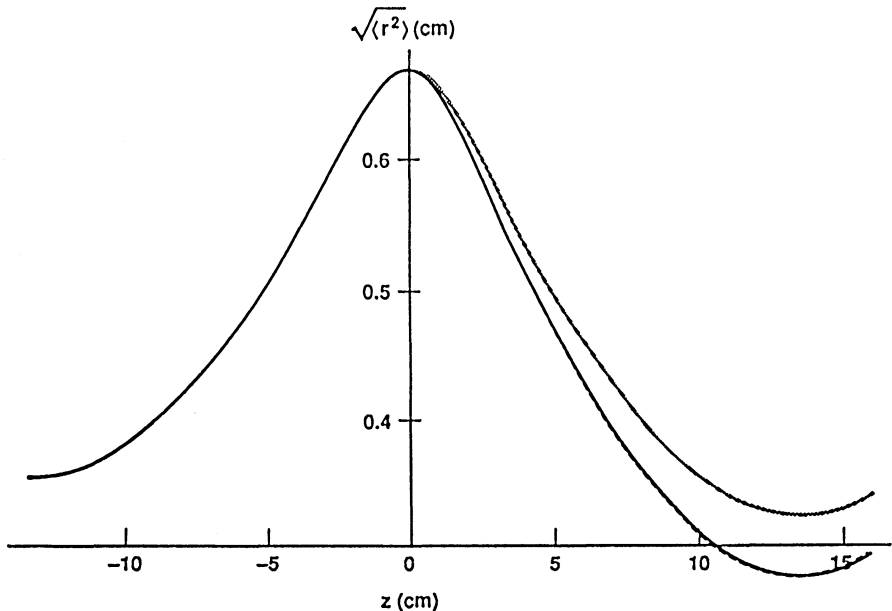


FIGURE 7 Plots of  $\sqrt{\langle r^2 \rangle}$  as a function of  $z$  with  $B_0 = 103$  G. The solid curve was obtained using SOLMAP. The dashed curve (which is hard to see because it is nearly identical to the solid curve) was obtained using a particle simulation. The light gray curve was obtained using SOLMAP but with the nonlinear part of the mapping omitted.

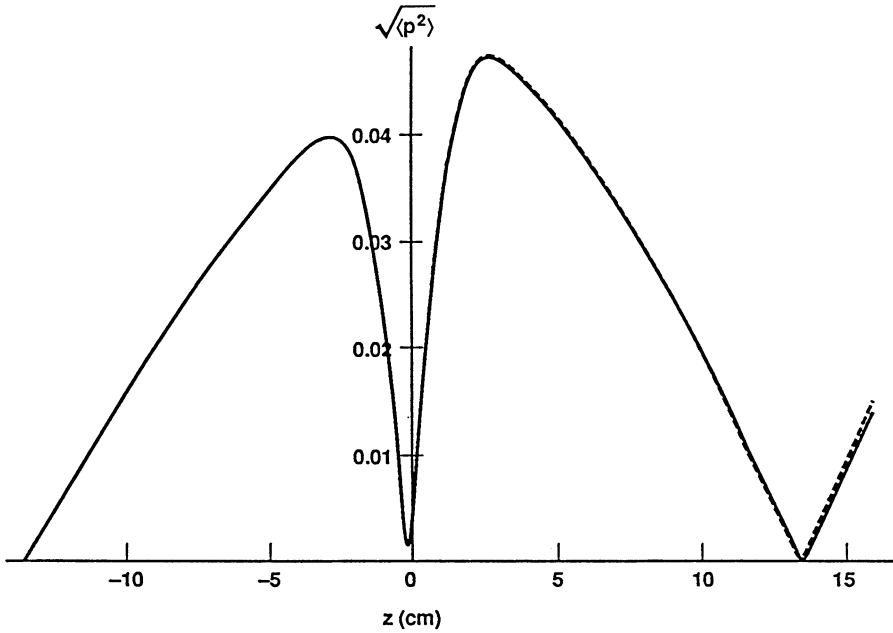


FIGURE 8 Plots of  $\sqrt{\langle p^2 \rangle}$  as a function of  $z$  with  $B_0 = 103$  G. The solid curve was obtained using SOLMAP. The dashed curve was obtained using a particle simulation.

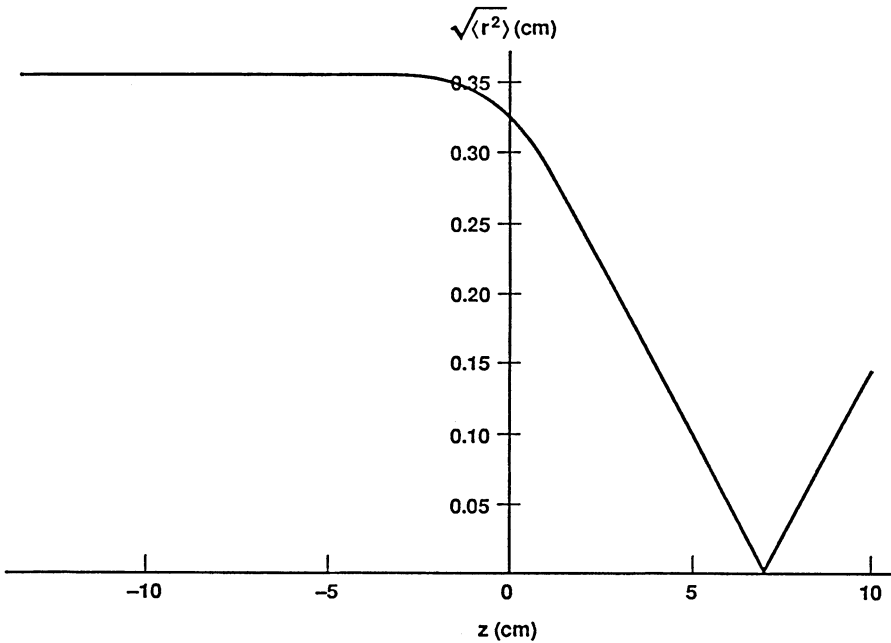


FIGURE 9 Plots of  $\sqrt{\langle r^2 \rangle}$  as a function of  $z$  with  $B_0 = 103$  G. Space charge forces have been neglected. (The transfer map results and the particle simulation results are indistinguishable.)

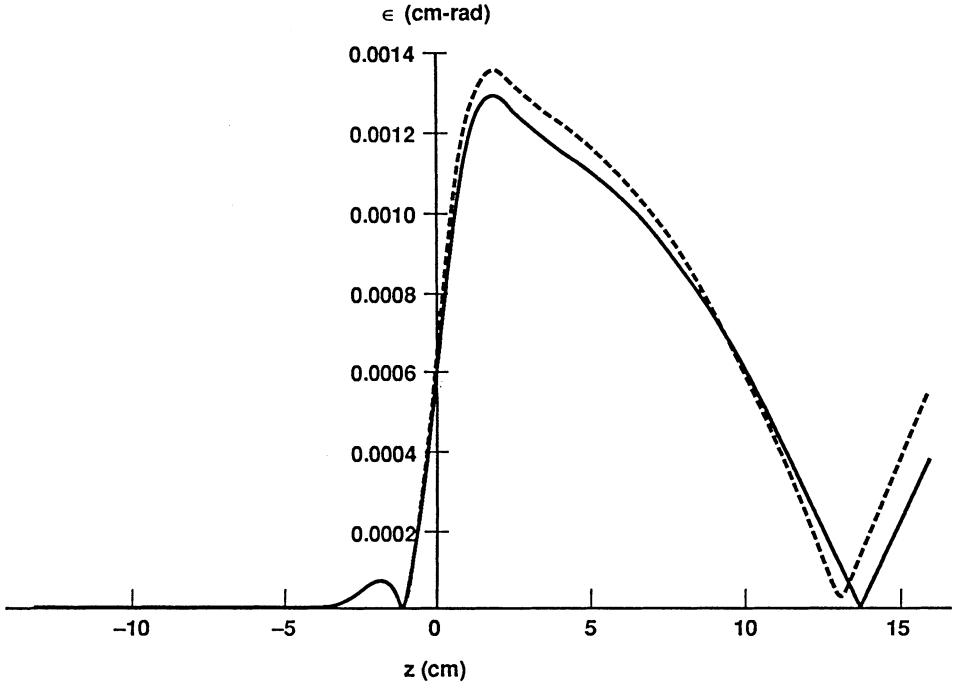


FIGURE 10 Plots of  $\varepsilon$  as function of  $z$  with  $B_0 = 103$  G. The solid curve was obtained using SOLMAP. The dashed curve was obtained using a particle simulation.

from the solenoid, we would have found progressively worse agreement. This is because the map  $\mathcal{M}$  and the approximations used to obtain it become invalid under certain circumstances. The limitations of our approach are discussed below.

## 10 DISCUSSION

Our approach is subject to certain limitations. This is due to the fact that our method is a perturbative method; it is based on the analysis of trajectories near a design trajectory through some fixed order. These limitations are not exclusive to our approach. In fact, *all* the usual transfer map codes (TRANSPORT, MARYLIE, etc.) suffer from this limitation. However, in the absence of space charge this is often of little concern since the standard beamline elements have fields that can be accurately described by a few terms in a power series.

In contrast, the halo of a charged particle beam has fields that are poorly described by a power series. Thus, our approach is less applicable to the analysis of a beam with a substantial halo, though one could still analyze the core of the beam.

Another limitation suffered by SOLMAP (as well as other transfer map codes) is that a third order representation of  $\mathcal{M}$  will not provide a valid description of the beam dynamics indefinitely, even if the forces are linear and cubic. This is because a



$z$ -dependent low order nonlinearity will produce indefinitely high order terms in the transfer map. Eventually, these terms cannot be neglected. Conventional transfer map codes that are used to analyze circular machines and periodic focusing systems deal with this problem by using tracking: the map  $\mathcal{M}$  for one period of the system is applied many times to obtain the state of particles after many periods. For our situation we cannot do this in general, because even though the external fields might be periodic, the self-fields (particularly the nonlinear term  $\phi_4$ ) might not be.

By construction, our method will be most useful for studying beams that have a density of the form

$$\rho(r, z) = a(z) + b(z)r^2. \quad (91)$$

Neglecting the  $z$ -dependence in calculating the scalar potential (as is customary in two-dimensional codes), the potential of such a beam contains terms proportional to  $r^2$  and  $r^4$ , as originally postulated. If Eq. (91) is valid over a large fraction of the beam, then  $\mathcal{M}$  will likely provide an accurate description of the beam dynamics over a large fraction of the beam. If Eq. (91) is only valid in the core, then  $\mathcal{M}$  will only be valid in the beam core.

The major advantage of self-consistent transfer maps is that this approach provides for the *direct* calculation of optical quantities such as aberration coefficients. (Most optical quantities of interest are simply related to the coefficients of  $\mathcal{M}$ .) In contrast, aberration coefficients are extremely difficult to obtain using particle simulation: To do this, one would “extract” the aberration coefficients by examining the initial and final conditions of particles near the beam core. If the trajectories are too near the optic axis, then the motion will be dominated by linear behavior and the nonlinear effects will be “lost in the noise.” If the trajectories are too far from the axis, then nonlinear effects from several orders will affect the particle dynamics making it difficult to extract the aberrations order-by-order. Lastly, one would require a *very* large number of simulation particles to accurately calculate the self fields and trajectories in the beam core.

Finally, our approach is orders of magnitude faster than particle simulation, since it is based on the numerical integration of a small number of ordinary differential equations. However, due to the restrictions mentioned above, it is not as widely applicable as particle simulation methods.

## 11 CONCLUSION

We have discussed a new approach for doing magnetic optics calculations in the presence of space charge. Our approach is based on the computation of a self-consistent transfer map,  $\mathcal{M}$ . We have analyzed cylindrically symmetric beams with space charge propagating in beam transport systems consisting of drifts and solenoids. We have derived ordinary differential equations for a third order representation of  $\mathcal{M}$ . These equations form the basis of a new computer program called SOLMAP. We have used this program to study the focusing of an electron beam by a solenoid, where both nonlinear solenoid fields and nonlinear space charge fields are important.

In this example, we calculated the density profile, the mean squared radius, and the mean squared emittance growth of the electron beam. We obtained good agreement with numerical simulation. Since our approach is based on the calculation of a map (rather than individual trajectories), it is much faster than particle simulation. Furthermore, it provides for the *direct* computation of optical quantities such as aberration coefficients (since they are simply related to the coefficients of  $\mathcal{M}$ ). Finally, because our approach is based on transfer maps, it may improve our understanding of the transport of intense beams.

## ACKNOWLEDGEMENTS

One of the authors (R. R.) thanks P. Loschialpo for discussions of his electron beam transport experiment.

## REFERENCES

1. K. Brown *et al.*, TRANSPORT, a Computer Program for Designing Charged Particle Beam Transport Systems, Stanford Linear Accelerator Center report SLAC 91 (1977).
2. F. C. Iselin, *The MAD Program Reference Manual*, CERN report CERN-LEP-TH/85-15 (1985).
3. A. Dragt *et al.*, MAYRLIE 3.0—A Program for Nonlinear Analysis of Accelerator and Beamline Lattices, *IEEE Trans. Nucl. Sci.*, **NS-32**, 2311 (1985).
4. R. Ryne, Lie Algebraic Treatment of Space Charge, Ph.D. thesis, Dept. of Physics, University of Maryland (1987).
5. R. Ryne and A. Dragt, Numerical Computation of Transfer Maps Using Lie Algebraic Methods, in Proc. 1987 IEEE Particle Accelerator Conference **2**, 1081 (1987).
6. F. Neri, GENREC 5.0, a Program for Handling Rare Earth Cobalt Quadrupoles Through Fifth Order, Dept. of Physics Technical Report, University of Maryland (1989).
7. M. Berz, *Part. Accel.*, **24**, 109 (1989).
8. J. D. Lawson, *The Physics of Charged Particle Beams* (Clarendon Press, Oxford, 1977).
9. E. Forest, Lie Algebraic Methods for Charged Particle Beams and Light Optics, Ph.D. Thesis, Dept. of Physics, University of Maryland (1984).
10. A. Dragt and E. Forest, *Advances in Electronics and Electron Physics* **67**, P. Hawkes, ed., Academic Press (1986), p. 65.
11. A. Dragt *et al.*, Numerical Third-Order Transfer Map for a Solenoid, Dept. of Physics Technical Report, University of Maryland (1990).
12. A. Dragt, Lectures on Nonlinear Orbit Dynamics, *Physics of High Energy Particle Accelerators*, AIP Conf. Proc. **87**, R. A. Carrigan *et al.*, ed. (1982).
13. A. Dragt *et al.*, *Ann. Rev. Nucl. Part. Sci.*, **38**, 455 (1988).
14. A. Dragt and E. Forest, *J. Math. Phys.*, **24**, 2734 (1983).
15. S. Wolfram, *MATHEMATICA, a System for Doing Mathematics by Computer* (Addison-Wesley, 1988).
16. P. Loschialpo *et al.*, *J. Appl. Phys.*, **57**, 10 (1985).
17. M. Abramowitz and I. Stegun, *Handbook of Mathematical Functions* (Dover Publications, Inc., New York, 1972), chapter 25, p. 882.
18. It should be noted that a very precise, quantitative comparison with experiment is difficult due to uncertainty in the initial conditions of the beam. In particular, the location and radius of the beam waist between the cathode and the anode was not known. Based on measurements of the beam radius 8 cm and 10 cm downstream from the magnet center (with  $B_0 = 0$ ), we assumed that a parallel beam of radius 5 mm was launched 13.4 cm upstream of the magnet center.
19. Our definition differs from the usual definition of the emittance because of our choice of canonical variables. The usual definition involves moments of  $x, x', y, y'$ , whereas our definition involves moments of  $x, p_x, y, p_y$ . In either case, the emittance is a sensitive measure of nonlinear effects, since it is unchanged if  $\mathcal{M}$  is a linear map.

20. The calculation of  $\varepsilon$  is not as accurate as  $\langle r^2 \rangle^{1/2}$  and  $\langle p^2 \rangle^{1/2}$  because, in view of (90), we have only computed the first term of a series expansion of  $\varepsilon$ . Our calculation of  $\varepsilon$  differs from the correct value just as the linearized (that is, one-term) calculation of  $\langle r^2 \rangle^{1/2}$  differs from the correct value (see Figure 7). We have verified that this occurs in the absence of space charge also.

## APPENDIX A CALCULATION OF THE SCALAR POTENTIAL COEFFICIENTS $\phi_2$ AND $\phi_4$

The purpose of this appendix is to give the details of the calculation of the coefficients  $\phi_2$  and  $\phi_4$  that are shown in Eqs. (73) and (74).

Consider a beam characterized by an initial distribution function

$$f^o(x, p_x, y, p_y) = \frac{1}{2\pi\lambda^2} e^{-(p_x^2 + p_y^2)/2\lambda^2} \rho^o(x, y), \quad (\text{A.1})$$

where

$$\int_{-\infty}^{\infty} \int_{-\infty}^{\infty} dx dy \rho^o(x, y) = 1. \quad (\text{A.2})$$

Let  $\zeta$  denote the collection  $(x, p_x, y, p_y)$ . The  $z$ -dependent distribution function is given by

$$f(\zeta) = f^o(\mathcal{M}^{-1}\zeta), \quad (\text{A.3})$$

where  $\mathcal{M}$  is the transfer map between  $z^i$  and  $z^f$ ,

$$\zeta^f = \mathcal{M}\zeta^i. \quad (\text{A.4})$$

Let  $\mathcal{M}$  be given by

$$\mathcal{M} = e^{i g_4} e^{i g_2}, \quad (\text{A.5})$$

where  $e^{i g_2}$  has the matrix representation

$$e^{i g_2} \sim M^o R = \begin{pmatrix} a & b & 0 & 0 \\ c & d & 0 & 0 \\ 0 & 0 & a & b \\ 0 & 0 & c & d \end{pmatrix} R, \quad (\text{A.6})$$

and where the polynomial  $g_4$  is given by

$$g_4 = e_1(p^2)^2 + e_2 p^2(r \cdot p) + e_3 p^2(r \times p)_z + e_4(r \cdot p)^2 + e_5(r \cdot p)(r \times p)_z + e_6 r^2 p^2 + e_7 r^2(r \cdot p) + e_8 r^2(r \times p)_z + e_9(r^2)^2. \quad (\text{A.7})$$

In the above expression,  $R$  is a rotation matrix and will play no role in the calculation of the scalar potential due to cylindrical symmetry.

As stated previously, the scalar potential is given formally by the following expression:

$$\psi(x, y; z) = \frac{\lambda_q}{(2\pi)^2 \varepsilon_0} \int d^4 \zeta' \int d^2 k \frac{1}{k^2} e^{ik_x(x-x')} e^{ik_y(y-y')} f^o(\mathcal{M}^{-1}\zeta'). \quad (\text{A.8})$$

Since  $\mathcal{M}$  is a symplectic mapping, its Jacobian determinant equals 1. It follows that

$$\psi(x, y; z) = \frac{\lambda_q}{(2\pi)^2 \varepsilon_0} \int d^4 \zeta' \int d^2 k \frac{1}{k^2} e^{ik_x(x - \mathcal{M}x')} e^{ik_y(y - \mathcal{M}y')} f^o(\zeta'). \quad (\text{A.9})$$

Thus we need to calculate  $\mathcal{M}x'$  and  $\mathcal{M}y'$ . Neglecting the rotation matrix, it follows that

$$\begin{aligned} \mathcal{M}x &\cong ax + bp_x + [g_4, ax + bp_x], \\ \mathcal{M}y &\cong ay + bp_y + [g_4, ay + bp_y], \end{aligned} \quad (\text{A.10})$$

where  $[, ]$  denotes the Poisson bracket and where we have neglected terms beyond third order. Expanding the exponential function in Eq. (A.9), we obtain

$$\begin{aligned} \psi(x, y; z) &\cong \frac{\lambda_q}{(2\pi)^2 \varepsilon_0} \int d^4 \zeta' \int d^2 k \frac{1}{k^2} \left( \frac{1}{2\pi\lambda^2} \right) e^{-(p_x'^2 + p_y'^2)/2\lambda^2} \rho^o(x', y') e^{i(k_x x + k_y y)} \\ &\quad \times e^{-ik_x(ax' + bp_x')} e^{-ik_y(ay' + bp_y')} \{1 - ik_x[g_4, ax' + bp_x'] - ik_y[g_4, ay' + bp_y']\}. \end{aligned} \quad (\text{A.11})$$

First we will perform the integrations over the variables  $p_x'$  and  $p_y'$ . The expression  $1 - ik_x[g_4, ax + bp_x] - ik_y[g_4, ay + bp_y]$  is a polynomial containing terms of the form  $p_x^m p_y^n$ , with  $m + n \leq 3$ . Thus, the integrals over  $p_x'$  and  $p_y'$  are simply Gaussian integrals. The resulting expressions will all contain a factor of  $2\pi\lambda^2 e^{-\lambda^2 b^2 (k_x^2 + k_y^2)/2}$ . We obtain

$$\begin{aligned} \psi(x, y; z) &= \frac{\lambda_q}{(2\pi)^2 \varepsilon_0} \iint dx' dy' \int d^2 k \frac{1}{k^2} e^{i(k_x x + k_y y)} e^{-\lambda^2 b^2 (k_x^2 + k_y^2)/2} \\ &\quad \times \rho^o(x', y') e^{-ia(k_x x' + k_y y')} P_3(x', y'), \end{aligned} \quad (\text{A.12})$$

where  $P_3(x, y)$  is a polynomial containing terms of the form  $x^m y^n$ , with  $m + n \leq 3$ . Equivalently, we can collect the terms containing  $x'$  and  $y'$  and write

$$\psi(x, y; z) = \frac{\lambda_q}{(2\pi)^2 \varepsilon_0} \int d^2 k \frac{S}{k^2} e^{i(k_x x + k_y y)} e^{-\lambda^2 b^2 (k_x^2 + k_y^2)/2}, \quad (\text{A.13})$$

where

$$S = \sum_{m+n \leq 3} c_{mn} \iint dx' dy' e^{-ia(k_x x' + k_y y')} \rho^o(x', y') x'^m y'^n, \quad (\text{A.14})$$

and where all the  $c_{mn}$  are independent of  $x'$  and  $y'$ . Now define the quantities  $W_{mn}$  according to

$$W_{mn} = \iint dx' dy' e^{-ia(k_x x' + k_y y')} \rho^o(x', y') x'^m y'^n. \quad (\text{A.15})$$

Since  $\rho^o$  has cylindrical symmetry, it follows that  $W_{00}$  is given

$$W_{00} = 2\pi \int_0^\infty dr r J_0(akr) \rho^o(r). \quad (\text{A.16})$$

Thus,  $W_{00}$  is a function of  $k = \sqrt{k_x^2 + k_y^2}$  only (and not of  $k_x$  and  $k_y$  separately). Let

$$h(k) = W_{00}. \quad (\text{A.17})$$

Then a straightforward calculation leads to the following relations:

$$\begin{aligned} W_{00} &= h(k), \\ W_{10} &= \frac{i \cos \theta}{a} h', \\ W_{01} &= \frac{i \sin \theta}{a} h', \\ W_{20} &= -\frac{\sin^2 \theta}{a^2 k} h' - \frac{\cos^2 \theta}{a^2} h'', \\ W_{11} &= \cos \theta \sin \theta \left( \frac{h'}{a^2 k} - \frac{h''}{a^2} \right), \\ W_{02} &= -\frac{\cos^2 \theta}{a^2 k} h' - \frac{\sin^2 \theta}{a^2} h'', \\ W_{30} &= (3i \cos \theta \sin^2 \theta) \left( \frac{h'}{a^3 k^2} - \frac{h''}{a^3 k} \right) - \frac{i \cos^3 \theta}{a^3} h''', \\ W_{21} &= (3i \sin^3 \theta - 2i \sin \theta) \left( \frac{h'}{a^3 k^2} - \frac{h''}{a^3 k} \right) - \frac{i \cos^2 \theta \sin \theta}{a^3} h''', \\ W_{12} &= (3i \cos^3 \theta - 2i \cos \theta) \left( \frac{h'}{a^3 k^2} - \frac{h''}{a^3 k} \right) - \frac{i \cos \theta \sin^2 \theta}{a^3} h''', \\ W_{03} &= (3i \cos^2 \theta \sin \theta) \left( \frac{h'}{a^3 k^2} - \frac{h''}{a^3 k} \right) - \frac{i \sin^3 \theta}{a^3} h''', \end{aligned} \quad (\text{A.18})$$

where

$$\begin{aligned} k_x &= k \cos \theta, \\ k_y &= k \sin \theta, \end{aligned} \quad (\text{A.19})$$

and where a prime denotes differentiation with respect to  $k$ .

Now apply the above substitutions to Eq. (A.14) for  $S$ . Because of cylindrical symmetry, the  $W_{mn}$  combine in such a way that the resulting expression for  $S$  does not involve  $\cos \theta$  or  $\sin \theta$ . That is,  $S$  is a function of  $k$  only, and  $S$  is given by

$$\begin{aligned} a^3 k S(k) &= a^3 k h + 4\lambda^4 a^3 b (4ae_1 - be_2) k^3 h - \lambda^6 a^3 b^3 (4ae_1 - be_2) k^5 h - (ae_7 - 4be_9) h' \\ &\quad + \lambda^2 a [b^2 e_7 + 2ab(e_4 + e_6) - 4a^2 e_2] k^2 h' \\ &\quad + \lambda^4 a^2 b^2 [3ae_2 - 2b(e_4 + e_6)] k^4 h' + (ae_7 - 4be_9) k h'' \\ &\quad + \lambda^2 ab [3be_7 - 2a(e_4 + e_6)] k^3 h'' + (ae_7 - 4be_9) k^2 h'''. \end{aligned} \quad (\text{A.20})$$

Rewriting Eq. (A.13), we obtain

$$\psi(x, y; z) = \frac{\lambda_q}{(2\pi)^2 \epsilon_0} \iint d\theta dk \frac{S(k)}{k} e^{ik(x \cos \theta + y \sin \theta)} e^{-(\lambda^2 b^2 k^2 / 2)}. \quad (\text{A.21})$$

Now we can perform the integral over  $\theta$ . The resulting expression is given by

$$\psi(x, y; z) = \frac{\lambda_q}{2\pi \epsilon_0} \int dk J_0(kr) \frac{S(k)}{k} e^{-uk^2}, \quad (\text{A.22})$$

where we have set

$$u = \frac{\lambda^2 b^2}{2}. \quad (\text{A.23})$$

Also, it follows that

$$E = -\frac{\partial \psi}{\partial r} = \frac{\lambda_q}{2\pi \epsilon_0} \int dk J_0(kr) S(k) e^{-uk^2}, \quad (\text{A.24})$$

$$\rho = -\epsilon_0 \frac{1}{r} \frac{\partial}{\partial r} \left( r \frac{\partial \psi}{\partial r} \right) = \frac{\lambda_q}{2\pi} \int dk k J_0(kr) S(k) e^{-uk^2}. \quad (\text{A.25})$$

At this point, we can expand  $J_0(kr)$  as a power series in  $r$  since we are only interested in obtaining a series expansion for  $\psi$ . We obtain

$$\phi_2 = -\frac{1}{2} \int dk e^{-uk^2} k S(k), \quad (\text{A.26})$$

$$\phi_4 = \frac{1}{32} \int dk e^{-uk^2} k^3 S(k), \quad (\text{A.27})$$

where

$$\psi = \frac{\lambda_q}{4\pi \epsilon_0} (\phi_2 + \phi_4 + \dots), \quad (\text{A.28})$$

and where we have dropped the constant term  $\phi_0$ . It is clear that, if we treat  $\phi_2$  and  $\phi_4$  as functions of  $u$ , then

$$\phi_4 = \frac{1}{16} \frac{\partial \phi_2(u)}{\partial u} \Big|_{u=\lambda^2 b^2 / 2}. \quad (\text{A.29})$$

Thus, all that is really needed is to calculate  $\phi_2(u)$ ; we can calculate  $\phi_4$  by differentiating the resulting formula.

Considering Eqs. (A.20) and (A.26), it is clear that  $\phi_2$  is of the form

$$\phi_2 = \sum c_m^n \int dk e^{-uk^2} k^m h^{(n)}(k). \quad (\text{A.30})$$

Let the quantities  $R_m^n$  be defined according to

$$R_m^n = \int_0^\infty dk e^{-uk^2} k^m h^{(n)}(k). \quad (\text{A.31})$$

Note that  $R_1^0$ , which we shall denote  $R(u)$ , is given by

$$R(u) = R_1^0 = \frac{\pi}{u} \int_0^\infty dr r \rho^o(r) e^{-(a^2 r^2/4u)}, \quad (\text{A.32})$$

where we have used the relation

$$\int_0^\infty dk k J_0(akr) e^{-uk^2} = \frac{1}{2u} e^{-(a^2 r^2/4u)}. \quad (\text{A.33})$$

By taking derivatives with respect to  $u$ , and by appropriate integrations by parts, it is possible to show that all of the  $R_m^n$  can be expressed in terms of  $R(u)$  and derivatives of  $R$ . In particular, the following relations hold:

$$\begin{aligned} R_1^0 &= R, \\ R_3^0 &= -R', \\ R_5^0 &= R'', \\ R_0^1 &= 2uR - 1, \\ R_2^1 &= -2R - 2uR', \\ R_4^1 &= 4R' + 2uR'', \\ R_1^2 &= -6uR - 4u^2R' + 1, \\ R_3^2 &= 6R + 14uR' + 4u^2R'', \\ R_2^3 &= 24uR + 36u^2R' + 8u^3R'' - 2, \end{aligned} \quad (\text{A.34})$$

where a prime denotes differentiation with respect to  $u$ . Substituting (A.20) and (A.34) into (A.26) we obtain the following for  $\phi_2$ :

$$\begin{aligned} -2a^3\phi_2(u) &= \{a^3 + 8a\lambda^2(a^2e_2 - 2ab(e_4 + e_6) + 2b^2e_7) + 16u(ae_7 - 4be_9)\}R(u) \\ &\quad + 8\{a^2b\lambda^4(2a(be_2 - ae_1) - b^2(e_4 + e_6)) + 4u^2(ae_7 - 4be_9)\} \\ &\quad + \lambda^2au(a^2e_2 - 4ab(e_4 + e_6) + 5b^2e_7)\}R'(u) \\ &\quad + \{a^3b^3\lambda^6(be_2 - 4ae_1) + 2a^2b^2\lambda^4u(3ae_2 - 2b(e_4 + e_6)) \\ &\quad + 4ab\lambda^2u^2(3be_7 - 2a(e_4 + e_6)) + 8u^3(ae_7 - 4be_9)\}R''(u) \end{aligned} \quad (\text{A.35})$$

Evaluating this expression with  $u = \lambda^2 b^2/2$  yields Eq. (73) for  $\phi_2$ . Making use of Eq. (A.29), we obtain Eq. (74) for  $\phi_4$ .

Lastly, we note that for an initially uniform beam given by

$$\rho^o(r) = \frac{1}{\pi\sigma^2} \begin{cases} 1 & \text{if } r \leq \sigma \\ 0 & \text{elsewhere} \end{cases}, \quad (\text{A.36})$$

the quantity  $h(k)$  is given by

$$h(k) = 2 \frac{J_1(ak\sigma)}{ak\sigma}, \quad (\text{A.37})$$

and  $R(u)$  is given by

$$R(u) = \frac{2}{a^2\sigma^2} (1 - e^{-(a^2\sigma^2/4u)}). \quad (\text{A.38})$$

## APPENDIX B DETAILS OF A PARTICLE SIMULATION PROGRAM

We have developed a particle simulation program to check our calculations based on self-consistent transfer maps. The simulation is based on a Hamiltonian formulation in cylindrical coordinates.

The relativistic Hamiltonian in cylindrical coordinates is given by

$$H = \sqrt{m^2c^4 + c^2(p_r - qA_r)^2 + c^2(p_\theta/r - qA_\theta)^2 + c^2(p_z - qA_z)^2} + q\psi, \quad (\text{B.1})$$

where

$$\begin{aligned} p_r &= \gamma m \dot{r} + qA_r, \\ p_\theta &= \gamma m r^2 \dot{\theta} + qA_\theta, \\ p_z &= \gamma m \dot{z} + qA_z, \end{aligned} \quad (\text{B.2})$$

and where a dot denotes  $d/dt$ . As in the text, we will now perform several transformations of this Hamiltonian (and we will use the symbols  $H$  and  $K$  to denote various Hamiltonians during this process). Following the standard procedure we can make  $z$  the independent variable. First set  $p_t = -H$  and solve for  $p_z$ . Then set  $K = -p_z$ . The quantity  $K$  is the new Hamiltonian with  $z$  as the independent variable:

$$K = -\sqrt{(p_t + q\psi)^2/c^2 - m^2c^2 - (p_r - qA_r)^2 - (p_\theta/r - qA_\theta)^2} - qA_z. \quad (\text{B.3})$$

Next define dimensionless variables according to the rules

$$\begin{aligned} \bar{r} &= r/l, & \bar{p}_r &= p_r/p^o, \\ \bar{\theta} &= \theta, & \bar{p}_\theta &= p_\theta/(p^o l), \\ \bar{t} &= t/(l/c), & \bar{p}_t &= p_t/(p^o c), \end{aligned} \quad (\text{B.4})$$

where  $l$  is any scale length and  $p^o$  is any scale momentum. Lastly go to the design trajectory by setting

$$\begin{aligned} R &= \bar{r}, & P_r &= \bar{p}_r, \\ \theta &= \bar{\theta}, & P_\theta &= \bar{p}_\theta, \\ T &= \bar{t} - \bar{t}^g, & P_t &= \bar{p}_t - \bar{p}_t^g, \end{aligned} \quad (\text{B.5})$$



where  $\bar{t}^g$  and  $\bar{p}_t^g$  denote quantities on a (generally  $z$ -dependent) “given” reference trajectory,  $r = 0$ . The Hamiltonian governing  $(R, P_r, \theta, P_\theta, T, P_t)$  is given by

$$H = -\frac{1}{l} \sqrt{\left(P_t + \bar{p}_t^g + \frac{q\psi}{p^o c}\right)^2 - \left(\frac{mc}{p^o}\right)^2 - \left(P_r - \frac{q}{p^o} A_r\right)^2 - \left(P_\theta/R - \frac{q}{p^o} A_\theta\right)^2} - \frac{q}{p^o l} A_z - \frac{\partial \bar{t}^g}{\partial z} P_t + \frac{\partial \bar{p}_t^g}{\partial z} T, \quad (\text{B.6})$$

where

$$\mathbf{A} = \mathbf{A}(lR, \theta, (T + \bar{t}^g)l/c; z), \quad \psi = \psi(lR, \theta, (T + \bar{t}^g)l/c; z). \quad (\text{B.7})$$

Now suppose that all the fields are time-independent. Then the total energy,  $-p_t$ , is a constant, as is  $-\bar{p}_t$ :

$$-\bar{p}_t = \frac{\gamma mc^2}{p^o c} + \frac{q\psi}{p^o c} = \frac{\gamma}{\gamma^o \beta^o} + \frac{q\psi}{p^o c} = \text{constant}. \quad (\text{B.8})$$

We will suppose that all particles have the design energy, so that we can set

$$P_t = 0. \quad (\text{B.9})$$

It follows that

$$H = -\frac{1}{l} \sqrt{\left(\bar{p}_t^g + \frac{q\psi}{p^o c}\right)^2 - \left(\frac{mc}{p^o}\right)^2 - \left(P_r - \frac{q}{p^o} A_r\right)^2 - \left(P_\theta/R - \frac{q}{p^o} A_\theta\right)^2} - \frac{q}{p^o l} A_z. \quad (\text{B.10})$$

Next, suppose that the scalar potential on axis equals zero:

$$\psi(r = 0) = \psi^g = 0. \quad (\text{B.11})$$

Then the kinetic energy also has a constant value on axis,  $(\gamma^g - 1)mc^2$ . Let  $p^o$  be given by

$$p^o = \gamma^g m v^g. \quad (\text{B.12})$$

This leads to the result

$$\bar{p}_t^g = -1/\beta^g. \quad (\text{B.13})$$

Lastly, we will choose  $l = 1$  meter (and we will abuse notation by writing  $r$  in place of  $R$ ). It follows that

$$H = -\sqrt{1 - 2\frac{q\psi}{p^o v^o} + \left(\frac{q\psi}{p^o c}\right)^2 - \left(P_r - \frac{q}{p^o} A_r\right)^2 - \left(P_\theta/r - \frac{q}{p^o} A_\theta\right)^2} - \frac{q}{p^o} A_z. \quad (\text{B.14})$$

Now we will restrict ourselves to systems with cylindrical symmetry, and assume that all the electromagnetic potentials are independent of  $\theta$ . Also, suppose that  $A_r = 0$ .

Then Hamilton's equations for  $\theta$  and  $P_\theta$  yield

$$P_\theta = \text{constant},$$

$$\theta = \theta^i + \int_{z^i}^{z^f} dz \frac{\left(P_\theta - \frac{q}{p^o} r A_\theta\right)/r^2}{\sqrt{1 - 2 \frac{q\psi}{p^o v^o} + \left(\frac{q\psi}{p^o c}\right)^2 - P_r^2 - \left(P_\theta/r - \frac{q}{p^o} A_\theta\right)^2}}. \quad (\text{B.15})$$

Further, Hamilton's equations for  $r$  and  $P_r$  are given by

$$r' = \frac{P_r}{\sqrt{1 - 2 \frac{q\psi}{p^o v^o} + \left(\frac{q\psi}{p^o c}\right)^2 - P_r^2 - \left(P_\theta/r - \frac{q}{p^o} A_\theta\right)^2}},$$

$$P_r' = \frac{\left(P_\theta/r - \frac{q}{p^o} A_\theta\right)\left(P_\theta/r^2 + \frac{q}{p^o} \frac{\partial A_\theta}{\partial r}\right) - \frac{q}{p^o v^o} \frac{\partial \psi}{\partial r} + \left(\frac{q}{p^o c}\right)^2 \psi \frac{\partial \psi}{\partial r}}{\sqrt{1 - 2 \frac{q\psi}{p^o v^o} + \left(\frac{q\psi}{p^o c}\right)^2 - P_r^2 - \left(P_\theta/r - \frac{q}{p^o} A_\theta\right)^2}} + \frac{q}{p^o} \frac{\partial A_z}{\partial r}, \quad (\text{B.16})$$

where a prime denote  $d/dz$ .

All that remains is to specify the potentials. Let the external vector potential be given by

$$\frac{q}{p^o} A_\theta = \frac{q}{p^o} \left( \frac{B_o}{2} r - \frac{B_o''}{16} r^3 \right) = \alpha r - \frac{\alpha''}{8} r^3. \quad (\text{B.17})$$

Now consider the calculation of the self-fields in the particle simulation. Let  $N$  denote the number of macroparticles (cylindrical shells) in the simulation, and let

$$F_k = \frac{1}{N} \times (\text{the number of particles with } r \leq r_k) \quad (k = 1, \dots, N). \quad (\text{B.18})$$

By Gauss' law, the radial electric field at the  $k$ th particle is given by

$$E(r_k) = \frac{\lambda_q}{2\pi\epsilon_o r_k} F_k, \quad (\text{B.19})$$

where  $\lambda_q$  is the charge per unit length, and the scalar potential is given by

$$\psi(r) = - \int_0^r E(r') dr'. \quad (\text{B.20})$$

In our particle simulation program, we calculate the scalar potential from the electric field values at  $r_k$  using the trapezoidal rule:

$$\psi(r_1) = -\frac{1}{2} E(r_1) r_1,$$

$$\psi(r_k) = \psi(r_{k-1}) - \frac{1}{2} [E(r_k) + E(r_{k-1})] (r_k - r_{k-1}) \quad (k = 2, \dots, N). \quad (\text{B.21})$$

To calculate the self vector potential, we will neglect the variation of  $v_z$  with radius and write

$$A_z = \frac{\beta^o}{c} \psi. \quad (\text{B.22})$$

Lastly, define  $\tilde{E}(r_i)$  and  $\tilde{\psi}(r_i)$  according to

$$\begin{aligned} E(r) &= \frac{\lambda_q}{2\pi\epsilon_o} \tilde{E}(r), \\ \psi(r) &= \frac{\lambda_q}{2\pi\epsilon_o} \tilde{\psi}(r), \end{aligned} \quad (\text{B.23})$$

and note that

$$\left(\frac{q}{p^o c}\right) \frac{\lambda_q}{2\pi\epsilon_o} = (\gamma^o)^2 \beta^o K, \quad (\text{B.24})$$

where  $K$  is the generalized perveance. Putting it all together, we obtain

$$\begin{aligned} r' &= \frac{P_r}{\sqrt{1 - 2(\gamma^o)^2 K \tilde{\psi} + ((\gamma^o)^2 \beta^o K \tilde{\psi})^2 - P_r^2 - \left(P_\theta/r - \alpha r + \frac{\alpha''}{8} r^3\right)^2}}, \\ P_r' &= -(\beta^o \gamma^o)^2 K \tilde{E} \\ &+ \frac{\left(P_\theta/r - \alpha r + \frac{\alpha''}{8} r^3\right) \left(P_\theta/r^2 + \alpha - \frac{3\alpha''}{8} r^2\right) + (\gamma^o)^2 K \tilde{E} - ((\gamma^o)^2 \beta^o K)^2 \tilde{E} \tilde{\psi}}{\sqrt{1 - 2(\gamma^o)^2 K \tilde{\psi} + ((\gamma^o)^2 \beta^o K \tilde{\psi})^2 - P_r^2 - \left(P_\theta/r - \alpha r + \frac{\alpha''}{8} r^3\right)^2}}, \end{aligned} \quad (\text{B.25})$$

where

$$\begin{aligned} \tilde{E}(r_k) &= F_k/r_k \quad (k = 1, \dots, N), \\ \tilde{\psi}(r_1) &= -\frac{1}{2} \tilde{E}(r_1) r_1, \\ \tilde{\psi}(r_k) &= \tilde{\psi}(r_{k-1}) - \frac{1}{2} [\tilde{E}(r_k) + \tilde{E}(r_{k-1})] (r_k - r_{k-1}) \quad (k = 2, \dots, N). \end{aligned} \quad (\text{B.26})$$

Equations (B.25) and (B.26) are the basic equations used by our particle simulation program. The equations of motion were integrated numerically using an 11th-order Adams predictor-corrector algorithm that was started with a 7th-order Runge–Kutta algorithm. (Such high order algorithms were not really necessary for this study. However, the routines were available and known to be reliable because they had been used previously in careful Lie algebraic numerical studies.)

Lastly, for comparing particle simulation results with our transfer map results, it is necessary to convert between the two coordinate systems  $(x, p_x, y, p_y)$  and  $(r, P_r)$ .

Our starting point is the relations

$$\begin{aligned}x &= r \cos \theta, \\y &= r \sin \theta, \\p_x &= \frac{v_x}{v^0} + \frac{q}{p^0} A_x, \\p_y &= \frac{v_y}{v^0} + \frac{q}{p^0} A_y.\end{aligned}\tag{B.27}$$

(Recall that, following our notation in the text,  $p_x$  and  $p_y$  are the canonical momenta divided by the scale momentum  $p^0$ .) It is clear that to compute the right hand sides of the above expressions we need to calculate  $v_x/v^0$  and  $v_y/v^0$ . To accomplish this, note that

$$x' = \frac{dx}{dz} = \frac{dx}{dt} \frac{dt}{dz} = \frac{\dot{x}}{\dot{z}} = \frac{v_x}{v_z} = \frac{v_x/v^0}{v_z/v^0}.\tag{B.28}$$

and similarly for  $y'$ . But  $v_z/v^0$  is given by

$$\frac{v_z}{v^0} = \sqrt{(v/v^0)^2 - (v_x/v^0)^2 - (v_y/v^0)^2}.\tag{B.29}$$

It follows that

$$\begin{aligned}x' &= \frac{v_x/v^0}{\sqrt{(v/v^0)^2 - (v_x/v^0)^2 - (v_y/v^0)^2}}, \\y' &= \frac{v_y/v^0}{\sqrt{(v/v^0)^2 - (v_x/v^0)^2 - (v_y/v^0)^2}}.\end{aligned}\tag{B.30}$$

Inverting these equations, we obtain

$$\begin{aligned}v_x/v^0 &= \frac{x'(v/v^0)}{\sqrt{1 + x'^2 + y'^2}}, \\v_y/v^0 &= \frac{y'(v/v^0)}{\sqrt{1 + x'^2 + y'^2}}.\end{aligned}\tag{B.31}$$

We are almost finished. From the above, it is clear that we need to compute  $x'$  and  $y'$  in terms of  $r$  and  $P_r$ . This is easily accomplished, since

$$\begin{aligned}x' &= r' \cos \theta - r\theta' \sin \theta, \\y' &= r' \sin \theta + r\theta' \cos \theta,\end{aligned}\tag{B.32}$$

and since  $r'$  and  $\theta'$  are known in terms of  $r$  and  $P_r$  through Hamilton's equations. Lastly, to utilize Eq. (B.30) we need to calculate  $(v/v^0)$ . Note that, from Eqs.

(B.8), (B.9) and (B.13),

$$\frac{1}{\beta^o} = \frac{\gamma mc}{p^o} + (\gamma^o)^2 \beta^o K \tilde{\psi}. \quad (\text{B.33})$$

It follows that

$$v/v^o = \frac{\sqrt{(1 - (\beta^o \gamma^o)^2 K \tilde{\psi})^2 - 1/(\gamma^o)^2}}{\beta^o (1 - (\beta^o \gamma^o)^2 K \tilde{\psi})}. \quad (\text{B.34})$$

Putting it all together, we can calculate  $(x, p_x, y, p_y)$  in terms of  $(r, P_r, \theta, P_\theta)$ . In fact, to reduce computer memory requirements our simulation only integrates the equations for  $r$  and  $P_r$ . This is all that is required to compute  $x^2 + y^2$ ,  $p_x^2 + p_y^2$  and  $xp_x + yp_y$  for each particle using the simulation results, since these quantities are all rotationally invariant.